Artificially generated turbulence: A review of phycological nanocosm, microcosm, and mesocosm experiments

Russell N. Arnott[1], Mehdi Cherif[2], Lee D. Bryant[1], Danielle J. Wain[1,a,*]

[1]Department of Architecture and Civil Engineering, University of Bath, UK; [2]Department of Ecology and Environmental Sciences, Umea University, Sweden

*Corresponding author: danielle.wain@7lakesalliance.org

[a]Current affiliation: 7 Lakes Alliance, Belgrade Lakes, ME, USA

Abstract

Building on a summary of how turbulence influences biological systems, we reviewed key phytoplankton-turbulence laboratory experiments (after Peters and Redondo (1997) and Peters and Marrasé (2000)) to provide a current overview of artificial-turbulence generation methods and quantification techniques. This review found that most phytoplankton studies using artificial turbulence feature some form of quantification of turbulence; it is recommended to use turbulent dissipation rates (ε) for consistency with physical oceanographic and limnological observations. Grid-generated turbulence is the dominant method used to generate artificial turbulence with most experiments providing quantified ε values. Couette cylinders are also commonly used due to the ease of quantification, albeit as shear rates not ε. Dinoflagellates were the primary phytoplanktonic group studied due to their propensity for forming harmful algal blooms (HAB) as well as their apparent sensitivity to turbulence. This study found that a majority of experimental set-ups are made from acrylate

plastics that could emit toxins as these materials degrade under UV light. Furthermore, most cosm systems studied were not sufficiently large to accommodate the full range of turbulent length scales, omitting larger vertical overturns. Recognising that phytoplankton-turbulence interactions are extremely complex, the continued promotion of more interdisciplinary studies is recommended.

Keywords: phytoplankton, interactions, harmful algal blooms, dinoflagellates

DECLARATIONS

Funding: Funding for this work was provided by a UK Royal Society International Exchange Grant IES\R3\170070 awarded to D. Wain and M. Cherif. We also acknowledge the financial support of the Knut and Alice Wallenberg Foundation (d.nr. 2016.0083).

Conflicts of Interest: None

Data Availability: Not applicable

Code Availability: Not applicable

INTRODUCTION

Turbulence is a key physical characteristic of aquatic systems that has profound impacts on phytoplankton population dynamics. Many early studies of these complex biological-turbulence interactions (Figure 1) focussed upon the role of turbulence in homogenously redistributing phytoplankton species throughout the water column. Stably stratified water columns typically promote positively buoyant species, allowing them to access increased light levels and, in nearshore waters, nutrients trapped above the pycnocline associated with catchment runoff. This scenario is vastly generalised and broadly characterised; additional studies into the various biological-turbulence interactions have yielded a variety of complex feedback mechanisms (Figure 1).

To understand this array of interconnected feedback mechanisms and accurately predict how phytoplankton behave in a given environment, researchers frequently adopt one of two approaches. The first is to model a general phytoplankton population using either a single, idealised species (Ross and Sharples, 2007; Ross and Sharples, 2008) or a combination of idealised species, e.g., positively buoyant dinoflagellates against negatively buoyant diatoms (Huisman et al., 1999). The second approach is to artificially produce turbulence in a mesocosm facility (hereafter referred to as a cosm to include facilities across an array of sizes) and expose either a monoculture, a mixture of species, or a natural population to varying levels of turbulence (Peters and Redondo, 1997). It is the latter that this review focuses upon.

This review begins with an overview of biological-turbulence interactions, drawing upon key studies to highlight the complex relationship between phytoplankton and turbulence. Best practice is then discussed with regards to the experimental design of phytoplankton cosm studies. Building upon this, the main methods of artificial turbulence generation (grids, shaker tables, aeration and Couette cylinders are discussed and reviewed, with less-

commonly used methods included in Appendix 1. This review culminates with a discussion of the different techniques used to quantify turbulence in cosm experiments, with lesser-used techniques found in Appendix 2.

Note that this review is limited to studies involving phytoplankton in controlled laboratory settings and, to this end, omits observations of natural systems as well as biological-turbulence interaction studies on higher trophic organisms (e.g., zooplankton and fish larvae). A total of 102 publications were used to complete this review. For publications where more than one generation technique was used, these have been counted as separate (a total of 8). For single experiments that yielded multiple publications (a total of 14), these have been counted as a single study. A summary table of all publications used for this review can be found in Appendix 3.

Quantifying Turbulence in Aquatic Environments

Most aquatic environments are turbulent flows comprised of eddies of varying size. As a fluid is perturbed at the macroscale (e.g., by wind), the energy imparted to that fluid cascades down from larger to increasingly smaller eddies until is it dissipated by the viscosity of the water. When measuring turbulence, there are a number of different variables that can be used to quantify the turbulent field. If we consider the rate at which the kinetic energy dissipates due to viscous forcing (i.e., the rate of turbulence kinetic energy dissipation; ε), it is possible to quantify turbulence.

It is also possible to quantify turbulence via velocity shear. As a fluid flows past a surface, shear is generated as friction between the fluid and the surface causes a boundary layer. This layer diffuses away from the surface, perpendicular to the direction of the flow. At certain thresholds, the boundary layer can give way to vortex shedding as the flow switches from laminar to turbulent. Within the remit of this review, shear is only used to quantify

97 turbulence in studies that make use of Couette cylinders where shear flow is used to generate
98 turbulence inside the cylinder. For laboratory measurements to be comparable with those in
99 the field, it is thus recommended that turbulence values are reported as ε in units of m^2/s^3,
100 which are the more commonly reported field units across disciplines.
101
102 **Study Aim**
103 This review builds upon the seminal work of Peters and Redondo (1997) and
104 incorporates literature from over the subsequent 20-plus years in order to ascertain best
105 practice when it comes to laboratory-based turbulence-generation studies. There is clearly the
106 need for greater standardisation across turbulence studies to facilitate easier and more direct
107 comparisons between studies. Peters and Redondo (1997) originally set out to "*spark more*
108 *interdisciplinary science,*" aiming to support biologists by introducing them to the world of
109 turbulence.
110 As well as discussing the various methods of generating turbulence (along with
111 accompanied mathematical principles), Peters and Redondo (1997) made a key discovery: ε
112 generated in laboratory experiments can commonly be up to orders of magnitude higher than
113 the average level of ε typically observed in the oceanic surface-mixed layer ($\varepsilon = 10^{-5}$ m^2/s^3).
114 Many of the "classic" papers on the effects of turbulence on phytoplankton growth (White,
115 1976; Pollingher and Zemel, 1981; Savidge, 1981) actually made no attempt to quantify the
116 levels of turbulence to which their phytoplankton populations were exposed. Thankfully, as
117 this study area developed over time, practitioners retrospectively quantified their
118 experiments; it is now standard to include estimates of ε and/or other turbulence quantities (
119 Table *1*).
120 From descriptions of laboratory set-ups, Peters and Marrasé (2000) estimated that the
121 level of ε in some experiments could have been as high as 0.23 m^2/s^3. Results from

experiments with exaggerated levels of turbulence may have water-quality applications such as artificial mixing in reservoirs and bathing water (Kirke, 2001; Visser et al., 2016). However, if the purpose of the experiment is to accurately model a biological-physical system that would occur in a natural aquatic system, then it is crucial for the experimental set-up to be as representative as possible of the real world. It is highly prudent to correctly quantify the level of turbulence generated prior to commencing a study to ensure that experimental conditions are representative of the environment being replicated.

Table 1 - Comparison of the main turbulence-generation techniques taken from publications between 1953 to 2020 inclusive (n=102). As well as the number of publications associated with each technique, we also see the proportion of studies which include turbulence quantification. See also Figure 6 for a chronology of publications for different turbulence generation methods.

Turbulence generation method	**Quantified**	**Quantified Elsewhere**	**Unquantified**	**Total Studies**
Aeration	1	3	7	11
Couette	15	3	0	18
Grid	29	2	1	32
Shaker	6	9	4	19
Other	14	1	6	21

Biological-Turbulence Interactions

Turbulence can have a profound influence on individual cells, specific species, and community composition in many ways. Most simply, high levels of turbulence can cause mechanical destruction by detaching flagella (Pollingher and Zemel, 1981), directly impacting motility. Turbulence also acts as a mechanism by which to homogenously distribute positively buoyant, motile species throughout a water column or to resuspend negatively buoyant, non-motile species; this directly impacts cell access to the photic layer and/or the light climate to which a cell is exposed (Kiørboe, 1993; Visser et al., 2016). Thus, the turbulent regime of a water body can have a profound impact on the phytoplankton

145 community composition with corresponding effects further along the food web. To this end,
146 turbulence has been seen to increase both predator-prey encounter rates (Rothschild and
147 Osborn, 1988) and contact rates between parasites and phytoplankton cell hosts (Llaveria et
148 al., 2010).

149 At the cell level, turbulence can impact cell growth via altering rates of nutrient uptake
150 and exposure to light. Phytoplankton cells uptake nutrients from the surrounding water via
151 diffusion; reduced flow at the cell surface causes the water surrounding the cell (i.e., the
152 concentration boundary layer) to become nutrient depleted (Prairie et al., 2012) and replete
153 with waste (Lazier and Mann, 1989; Kiørboe, 1993). Turbulent flows are seen to increase the
154 laminar shear across the cell surface, eroding the concentration boundary layer and causing a
155 corresponding increase in nutrient flux to the cell (Lazier and Mann, 1989; Kiørboe, 1993;
156 Arin et al., 2002; Peters et al., 2006). Conversely, turbulence can also reduce the rate of cell
157 division (Sullivan et al., 2003) with prolonged exposure to high turbulence intensities
158 resulting in increased cell mortality (White, 1976; Pollingher and Zemel, 1981). Even short-
159 duration, high-intensity turbulence applied at a specific time in the cell cycle can inhibit cell
160 division (Pollingher and Zemel, 1981). Turbulence can also induce the "flashing light effect"
161 (a.k.a., the light–dark cycle, intermittent illumination, light intensity fluctuation and/or
162 dynamic light condition;(Sato et al., 2010)) in cells. This phenomenon has been observed to
163 increase the photosynthetic efficiency in cultured species exposed to intermittent light
164 fluctuations (Laws et al., 1983; Grobbelaar, 1989) via a reduction in photoinhibition (Nedbal
165 et al., 1996) thought to be linked to the light fluctuations that a cell would be exposed to
166 within a turbulent environment.

167 Turbulence also can cause changes in cell morphology. For example, the dinoflagellate
168 *Ceratocorys horrida* Stein experienced a reduction in cell size and spine length in response to
169 high turbulent intensities, an adaptation postulated to allow cells to sink below the more

turbulent conditions and reduce risk of mechanical damage (Zirbel et al., 2000). Cell morphology is also linked to light climate with elongated particles becoming aligned in the direction of flow, thereby increasing the backscatter of light in the water column (Guasto et al., 2012). Morphology is also linked to nutrient uptake, the rate of which preferentially increasing in larger cells when compared to smaller cells in turbulent conditions (Guasto et al., 2012).

Further studies linking turbulence to morphology and surface-area-to-volume (SAV) ratios across different species suggested these parameters to be crucial in determining nutrient uptake (Fraisse et al., 2015). Growth rate of large species was often exceeded by that of smaller species in nutrient-limited conditions (Cózar and Echevarría, 2005) whereas shape dictated how a species behaved hydrodynamically while in turbulent flows and whilst sinking (Padisák et al., 2003). Clearly, shape and SAV ratios are interlinked; elongated cells were seen to outcompete spherical cells with regards to nutrient acquisition (Pahlow et al., 1997).

Morphology also plays a key role in how colonial, chain-forming filamentous species interact with turbulent fields; for example, longer filaments sink faster in calm conditions, but under turbulent conditions a filament can grow to greater sizes as a result of turbulence-induced increases in light access (Fraisse et al., 2015). Chain-forming, postulated to be a means for avoiding grazing (Kiørboe, 1993), also provides a mechanism by which to increase form drag and thereby reduce sedimentation (Padisák et al., 2003). Turbulence has been observed to separate large colonies, thereby separating filament chains into smaller sections (Pahlow et al., 1997) which are able to sink and access additional nutrients at depth (Padisák et al., 2003). The ability of a colony to deform in different flow environments is thought to give colonial species a competitive advantage in a wider range of turbulent regimes (Guasto et al., 2012). Turbulence-enhanced nutrient uptake is also seen to preferentially affect colonies when compared to singular cells (Guasto et al., 2012). Chain-forming species exhibit

195 a range of lengths, orientations and flexibilities, all of which affect their hydrodynamic
196 properties. Compared to flexible chains, increasingly stiffer chains not only exhibit higher
197 rates of nutrient consumption but also experience larger nutrient fluxes (Musielak et al.,
198 2009). With focus on phytoplankton as a carbon pump, colonial diatoms are known to be
199 prolific fixers of carbon dioxide (CO_2) where under turbulent conditions, they export carbon
200 from the upper ocean to depths by forming fast-sinking aggregates. To this end, rates of
201 turbulence-enhanced carbon uptake have been observed to be higher in chain-forming species
202 than in individual cells (Bergkvist et al., 2018).

203 The traditional view of phytoplankton behaving as benign passengers at the whims of
204 forces within the water column holds for macroscale flows; however, the various experiments
205 described within this review act to showcase a dynamic group of organisms capable of
206 complex abilities and feedback mechanisms permitting them to gain a foothold over
207 competing species by altering their properties to suit the conditions of the water column.
208 Increasingly, researchers are recognising that different phytoplankton have an array of
209 ecological adaptations that allow them to prosper within an array of various turbulent
210 environments (Margalef, 1997; Fraisse et al., 2015). With emphasis placed on the effect of
211 turbulence, Figure 1 allows us to appreciate the complexity of turbulence-plankton
212 interactions. Further weight is added herein to recommendations found in key papers
213 (Margalef, 1997; Peters and Redondo, 1997) which characterise turbulence within a water
214 column to be as significant a biological determinant as temperature or salinity, thereby
215 emphasising the importance of measuring shifts in phytoplankton communities and
216 turbulence concurrently.

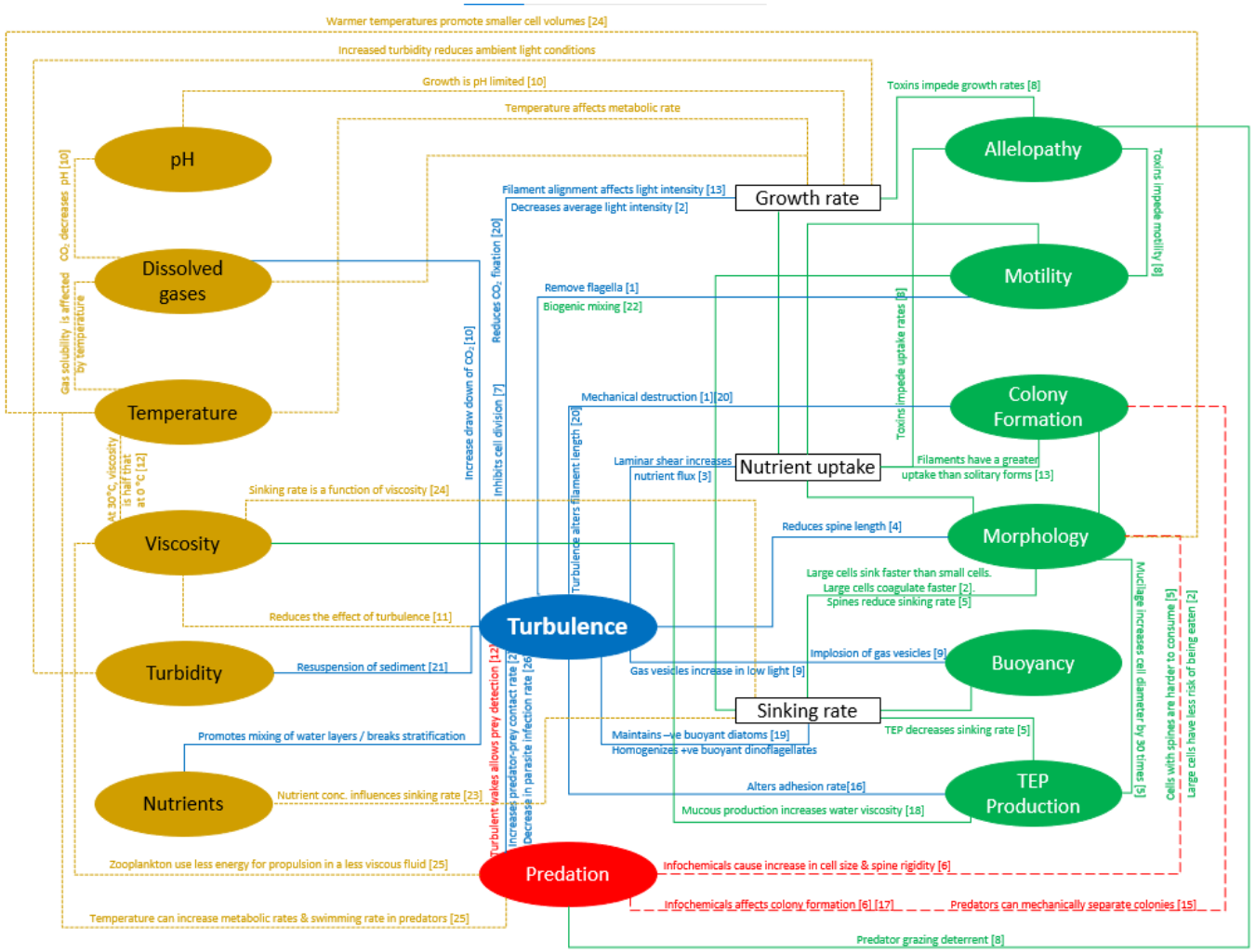

[1] Pahlow et al. (1997)
[2] Kiørboe (1993)
[3] Lazier and Mann (1989)
[4] Zirbel et al. (2000)
[5] Padisák et al. (2003)
[6] Lürling (1998)
[7] Pollingher and Zemel (1981)
[8] Schwartz et al. (2016)
[9] Walsby (1971)
[10] Havskum and Hansen (2006)
[11] Hellung-Larsen and Lyhne (1992)
[12] Margalef (1997)
[13] Guasto et al. (2012)
[14] Leterme et al. (2008)
[15] Dawidowicz (1990)
[16] Beauvais et al. (2006)
[17] Long et al. (2007)
[18] Smayda and Reynolds (2001)
[19] Huisman et al. (1999)
[20] Moisander et al. (2002)
[21] Visser et al. (2016)
[22] Katija (2012)
[23] Bienfang et al. (1982)
[24] Naselli-Flores et al. (2020)
[25] Simoncelli et al. (2019)
[26] Llaveria et al. (2010)

Figure 1 - Flow diagram summarising various links and feedbacks of phytoplankton-turbulence interactions. Green = biological characteristics; white = rates; blue = turbulence processes; red = predation; gold = water properties. Associated coloured text denotes the forcing factor for that link. Where appropriate, links are qualified with numbered references. Dashed lines are included to assist colour-blind readers in distinguishing problematic colours.

EXPERIMENTAL DESIGN

Facility Considerations

Before evaluating different methods of turbulence generation, the experimental vessel(s) itself should be considered as something as simple as the shape, scale and material can considerably influence the experiment if not properly accounted for. As such, the following section discusses the potential implications of tank volume, tank shape, the material the tank is constructed from and how the tank is filled.

Volume of Tank

Crossland and La Point (1992) posed the question: "*How big does a mesocosm have to be to provide a realistic simulation of the natural environment?*" The answer is very dependent on the scale and scope of study taking place. Throughout the literature, however, the terms nanocosm, microcosm and mesocosm are frequently used interchangeably. Whether a cosm is classed as nano-, micro-, or meso- is open to interpretation with some using volume as the distinguishing feature (Waller and Allen, 2008; Alexander et al., 2016) while others use diameter or length (Kangas and Adey, 2008). In summary, Solomon and Hanson (2014) provided the best characterisation of the different cosms (Table 2). Traditionally, researchers used small (< 1L) nanocosms described as "simplified, physical models of an ecosystem that enable controlled experiments to be conducted in the laboratory or in situ" (Matheson, 2008). Increasing in size leads sequentially to microcosm and mesocosm systems, generally described to be "bounded and partially enclosed outdoor experimental setups falling between laboratory microcosms and the large, complex real world macrocosms" (Odum, 1984). These facilities may be housed inside or outdoors (i.e., on land or in water) depending on the nature of the setup. For outside enclosures suspended within an aquatic environment, Solomon and

Table 2 - Characterisation of different cosms. After Solomon and Hanson (2014).

	Nanocosm	**Microcosm**	**Mesocosm**
Volume (L)	1 – 100	100 - 15000	>15000
No. of Trophic Levels	2	3+	3+
Optimum study duration	<8 weeks	<1 season	>1 season
Typical Location	Inside	Inside or outside	Outside

Hanson (2014) suggested the term 'limnocorral' to differentiate these from facilities on land while Parsons et al. (1978) opted for a controlled ecosystem enclosure.

With regards to biological studies, a larger experimental volume supports greater biodiversity and allows for a larger number of trophic levels to be observed concurrently (Alexander et al., 2016); conversely, smaller microcosms typically exclude higher trophic levels due to size constraints (Matheson, 2008). With regards to turbulence, vertical overturns are known to exist between 10^{-3} to 10^{1} m; while smaller cosms represent the smaller end of this range, clearly a much larger tank would be required in order to capture the upper range. After all, it is not possible to produce a 10 m vertical overturn if the tank itself is shallower than 10 m depth. Using cosm volume as an indicator of maximum turbulent overturn size within a particular experiment, a majority of studies were found to use fluid volumes smaller than 1 m^3 (Figure 2). As expected, it is larger volume limnocorral studies that make up a bulk of the experiments above this 1 m^3 threshold.

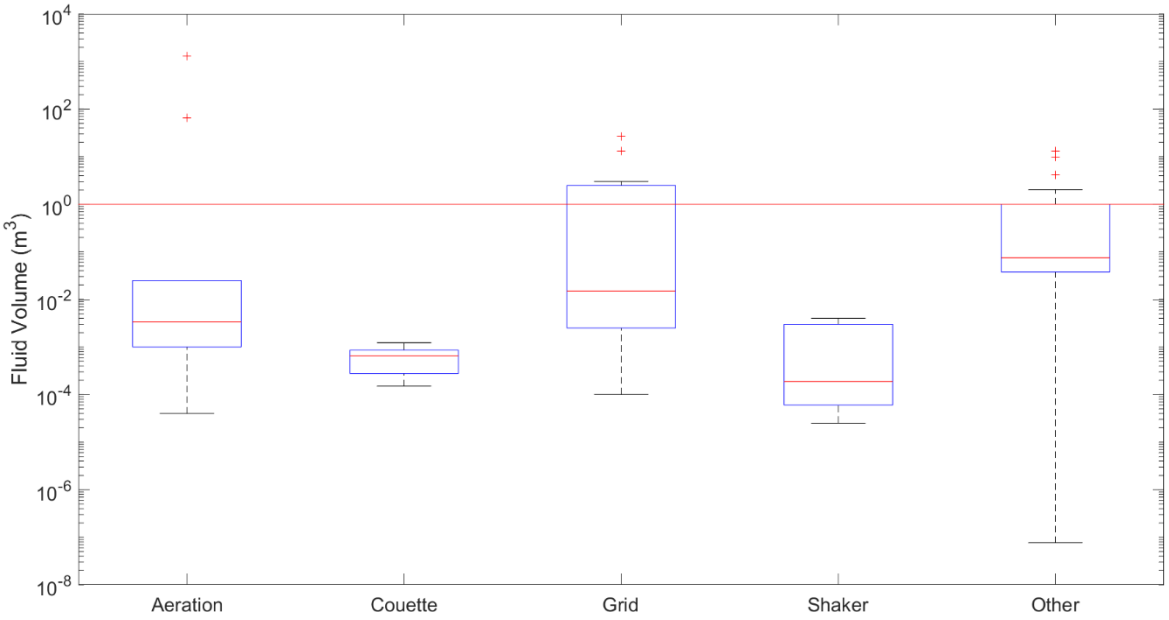

Figure 2 - Boxplots of approximate fluid volumes involved with different types of turbulence-generation experiments. Central line in each box is the median; top and bottom of each box indicate the 25th and 75th percentiles. Whiskers extend to the most extreme data points not considered outliers, with outliers plotted as plus-signs. Continuous horizontal line indicates a volume of 1 m³, considered to be the minimum volume required to capture realistic turbulence length scales Note the log scale on the y-axis.

Shape of Tank

Peters and Redondo (1997) put forth the assumption that biologists tend to use cylindrical tanks as, in theory, these display a higher degree of homogeneity. Conversely, physical studies are generally undertaken in cuboid tanks as the corners disrupt secondary flow effects; at the same time, modelling flow within square-based tanks is considered simpler mathematically. However, cuboid tanks are considered less homogenous overall due to the presence of corners (Peters and Redondo, 1997) which can cause 1) material to collect, 2) organisms to grow there and/or 3) changes in the turbulent field. In a comparison between turbulence generated in smooth- and baffled-bottom flasks, ε values were seen to be two orders of magnitude higher in the latter (Kaku et al., 2006). The shape of a tank can clearly play a significant role in the turbulence regime within.

Matheson (2008) acknowledged the importance of SAV ratio in microcosm design; those with a large SAV ratio can promote edge communities of biofilms or cause other organisms to congregate to avoid predation. As such, these biological "wall effects" can add significant bias into an experiment; efforts should hence be made to use facilities with small SAV ratios. The size and aspect ratios of the test vessel would be expected to affect the growth rate for many reasons. High-volume growth "ponds" (i.e., vessels with a shallow depth but increased exposed water surface area) are designed to maintain as much of the population in the photic layer as possible while also reducing the effects of shadowing. A larger exposed water surface area would not only increase gas exchange across the boundary but would also promote a higher evaporation rate.

Material of Tank

Vessels may be constructed out of an array of different materials depending on availability and size requirements. Firstly, it is essential that the material of the tank does not influence the fluid medium inside the tank. As such, it is not advised to use ferrous materials to construct mesocosms as not only does this add iron to the fluid medium (which is a photosynthesis-limiting micronutrient; (Martin and Michael Gordon, 1988) but the tank itself is also at risk of corrosion, especially if using saline fluid media.

Other materials may also cause micronutrients to be leached into the culture medium; glass has the potential to provide a source of silicon, known to be a limiting nutrient for diatoms (Kilham, 1971). Hellung-Larsen and Lyhne (1992) studied the effects of vessel material on the rates of cell division in the protozoan *Tetrahymena* sp. and observed no significant difference when using glass, siliconized glass and plastic.

With an increasing propensity for ecologists and other researchers to experiment with three-dimensional (3D) printing technology, it has been observed that certain extrusion

materials, particularly resins, remain toxic to aquatic organisms for some time. Should a microcosm tank be 3D-printed in resin, however, exposure to ultraviolet (UV) light can reduce its toxicity substantially (Behm et al., 2018).

Conversely, many cosms are constructed from artificial polymers such as acrylate, polyvinyl-chloride (PVC) and polycarbonate which all undergo photodegradation reactions under UV light (Yousif and Haddad, 2013), potentially releasing toxins that could adversely influence productivity. In a similar vein, the presence of polystyrene nanoplastics were seen to reduce the chlorophyll content of the diatom *Chaetoceros neogracilis* VanLandingham with subsequent implications on cellular growth and photosynthetic efficiency (Gonzalez-Fernandez et al., 2019). As such, it is crucial that the tank material itself is not influencing the growth rate of the organisms being studied. Some plastics are also permeable to certain gases; depending on the nature of the study, this should also be considered and may even be desirable (Matheson, 2008).

As well as releasing chemicals into tank water, certain cosm materials can absorb chemical species from the water (Kangas and Adey, 2008). Zhou et al. (2016) submerged Plexiglass tanks in water for 15 days prior to their experiment to allow the tanks to absorb and/or release any chemicals and equilibrate accordingly. Of the cosms studied, a third was comprised of plastics that undergo UV degradation (Figure 3). Another third was made of glass which may be correlated to the high proportion of studies using glass Couette cylinders and Pyrex vessels on shaker tables.

Typically, biologists cultivate cells in transparent vessels to maximise incident light that allows cells to reproduce further. This eliminates any light gradient within the tank that would be present in nature. As such, it is advised to use opaque materials when studying the effects of turbulence; this generates a light-gradient through the tank which can have a significant impact on results, especially when using phototactic or motile species or those

with the ability to regulate their buoyancy. It should also be noted that while surface shading is a natural phenomenon that regulates phytoplankton growth, light introduced through transparent walls is susceptible to biofilm growth resulting in decreased light levels over time (Matheson, 2008). Some practitioners have avoided this effect via a periodic scrubbing of the tank walls with a brush or similar (Zhou et al., 2016).

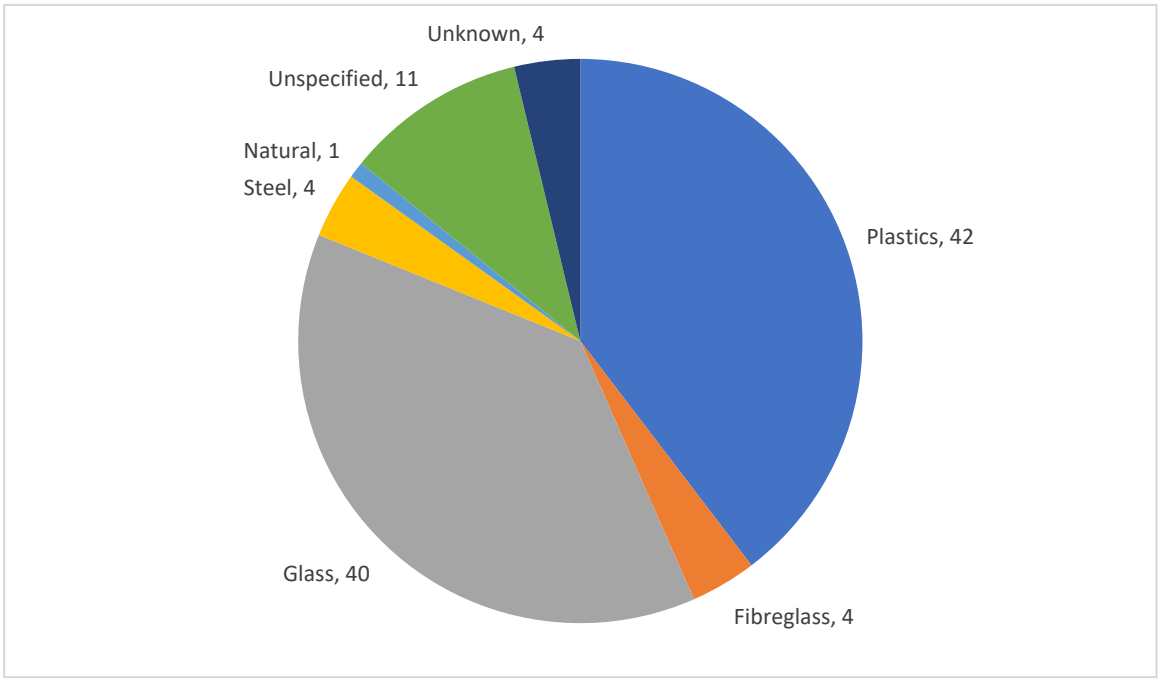

Figure 3 - Materials used in cosm design (based on n=102 studies). Plastics refers to tanks comprised of acylate, polycarbonate, polyethylene and polyvinyl chloride, all of which are known to undergo UV degradation. Glass refers to both standard glass and Pyrex. For cosms comprised of more than one material (n = 2), these materials have been counted separately.

Filling

Phytoplankton-turbulence studies that use smaller nano- and microcosms typically study the effects of one or two different species at a time based on seeding of the cosms with laboratory-cultivated cells grown in incubators. However, larger mesocosms and limnocorrals are typically used to look at natural planktonic communities that may be comprised of multiple trophic levels and organisms of different sizes. Land-based facilities are typically filled via pumping offshore waters from a particular depth into the enclosures (Båmstedt and

Larsson, 2018). Ideally, sets of cosms will be filled simultaneously or as close timed as possible to insure homogeneity across all replicate cosms. It is important that the pump filling system does not inadvertently preclude any larger species nor damage them in their transport through the pump system (Striebel et al., 2013). Some facilities are able to filter certain size fractions from the inflow water (Båmstedt and Larsson, 2018), thereby allowing e.g., microzooplankton through but omitting mesozooplankton that might graze upon certain size fractions or cause morphological changes via infochemicals (Long et al., 2007; Figure 1).

Environmental Variables

Having evaluated potential issues that may arise within different facilities, we next considered how environmental variables within the cosms may be influenced by particular experimental setups. Specifically, we looked at the implications of study duration, nature of the turbulence generated, light climate within the tank and general properties of the water itself.

Duration of study

As suggested by Table 2, the duration of a study is somewhat dictated by the volume of the tank, with larger facilities being able to accommodate a higher number of trophic levels (Solomon and Hanson, 2014). It stands to reason that any change in the turbulent regime within the tank will take time for its effects to cascade through a wider array of trophic communities. Depending on the rate of cell division across different species (and given conditions that promote or inhibit growth), it is expected that a phytoplanktonic community would adjust to a new turbulent regime within a few days. Given a minimum cell division rate of ~0.5 divisions per day (Banse, 1991), two days should account for cells to replicate at least once.

371 It is important to account for the effects of turbulence on growth due to changes in
372 light regime (Kiørboe, 1993), changes in cell division rate (Pollingher and Zemel, 1981) and
373 morphological changes to future generations (Zirbel et al., 2000). Once the new turbulent
374 regime is established and the community adjusts accordingly to the new physical
375 environment, ecological processes will dominate in regard to inter-species and trophic
376 interactions.
377
378 *Intensity or level of turbulence*
379 If the purpose of conducting laboratory experiments is to ascertain the effect(s) of
380 turbulence on a planktonic population, then it is crucial for the generated turbulence to
381 properly represent the real-world, naturally turbulent environment to which organisms would
382 be exposed. Using large, external limnocorrals may seem to be the easiest way to ensure that
383 the turbulence within a cosm is as natural as possible; however, it has been observed that
384 enclosing a portion of a water body within a cosm can significantly reduce the internal mixing
385 regime when compared to conditions immediately outside the enclosure (Striebel et al., 2013).
386 As well as the tendency to produce excessive and unrealistic levels of turbulence
387 within a cosm (Peters and Marrasé, 2000), there are a number of reasons to rethink existing
388 approaches to artificially generated turbulence. It is important to consider how turbulence
389 manifests itself within aquatic environments where turbulence is generally relatively weak.
390 Observations suggest that ε typically exists between 10^{-10} and 10^{-7} m^2/s^3, both in central ocean
391 systems (Fuchs and Gerbi, 2016) and freshwater lakes (Wüest and Lorke, 2003). While wind-
392 mixed and convectively mixed surface layers seldom exceed 10^{-5} m^2/s^3 in the open ocean, surf
393 zone ε values of up to 10^{-2} m^2/s^3 have been observed (Fuchs and Gerbi, 2016). Of the
394 experiments reviewed here, a majority focused on the upper range of ε found in natural
395 environments (Figure 4).

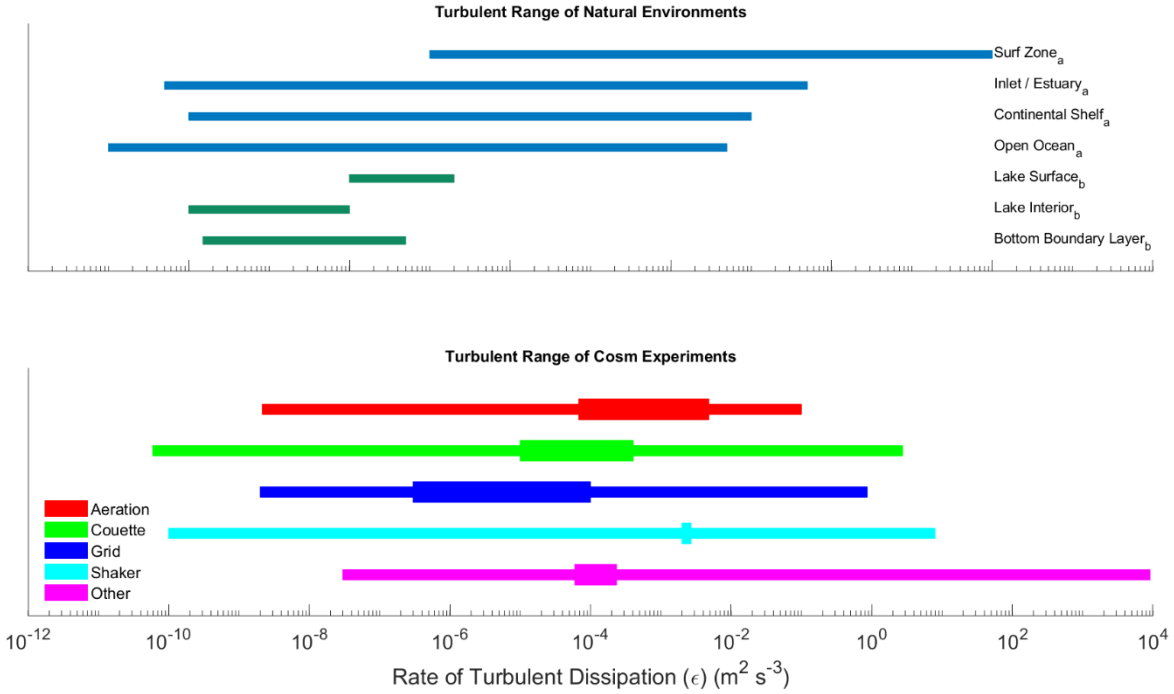

396

397 *Figure 4 – Upper: comparison of range of turbulent dissipation rates (ε) found in marine and*
398 *lacustrine environments taken from Fuchs and Gerbi (2016)($_a$) and Wüest and Lorke*
399 *(2003)($_b$) respectively. Lower: ε produced from turbulence-generation studies evaluated for*
400 *this review (n = 102). Horizontal lines span total ranges (thin lines) with the lower and upper*
401 *log-median ε limits (thick lines) for each generation method.*
402

403 In addition to being relatively weak, turbulence in natural environments can be highly
404 sporadic, both temporally and spatially (Waterhouse et al., 2014). Thus, laboratory
405 experiments that constantly force turbulence generation and aim for isotropic conditions
406 across relatively small tank volumes are unrepresentative of natural conditions. In particular,
407 direct and indirect turbulence avoidance strategies have been observed in planktonic
408 organisms at a number of trophic levels (Franks, 2001; Pringle, 2007). Thus, for a cosm to
409 properly represent the natural environment, a refuge region of less-turbulent water should be
410 incorporated into the experimental design to allow the organisms some respite from intense
411 turbulence and to facilitate natural behavior (Franks, 2001). It is thus recommended that
412 experimental designs of cosms need to be large enough to include this refuge region. While
413 this is thought to be particularly applicable to zooplankton studies, many motile

phytoplankton species position themselves within the water column to obtain light and/or nutrients and would also benefit from tank refuge regions.

Light

Many standard biological growth facilities are designed to maximise growth with regards to the light climate of the vessel. As mentioned previously, it is crucial for incident light within turbulence-generation tanks to attenuate with depth. The biological-turbulence interactions that underpin the critical depth hypothesis (Sverdrup, 1953) would be invalidated if light-levels did not attenuate with depth.

With regards to the light spectrum that organisms are exposed to, it is best to use direct sunlight to capture all spectrographic components of the sun at surface level. While this will be the natural default in outdoor facilities and limnocorrals, indoor facilities traditionally have relied on filament lamps that had a tendency to over-represent light within the infrared parts of the spectrum, causing heating to the cosm surface and various thermal lid effects (Båmstedt and Larsson, 2018). Conversely, filament lamps under-represent the UV component of sunlight and, while UV light is attenuated quickly in the water column, it can still have an influence on cosm ecology. For example, waters with high levels of coloured dissolved organic matter (CDOM) have been shown to increase the attenuation of visible light, thereby reducing the depth of the upper photic layer (Reynolds, 2009). CDOM preferentially absorbs visible light towards the blue end of the spectrum as well as UV. The UV light interacts with an array of complex compounds found in CDOM, causing them to decompose into smaller compounds which can more easily interact with other biochemical processes. Thus, the presence of CDOM in the water column can have a profound impact on primary productivity with depth (Coble, 2007). Paczkowska et al. (2017) showed the explicit link between CDOM and the phytoplanktonic community; as CDOM degrades in the

environment, it provides an important nutrient supply for heterotrophic bacteria which are a potential food source for any mixotrophic species. Furthermore, under the restricted light conditions associated with CDOM, phytoplankton respond by increasing the cellular concentration of the photosynthetic pigments, including chlorophyll-*a*. These restricted light conditions can also promote a shift towards species with smaller cell sizes (Paczkowska et al., 2017).

With the advent of halogen and LED lights, it is now easier to reproduce the surface sunlight spectrum within indoor cosms, accounting for UV, visible and infrared components accordingly. Care should still be taken to measure the photoactive radiation (PAR) within the cosm to ensure it is attenuating sufficiently with depth and is not too bright to cause photo-inhibition of cells. As for the duration of light exposure, it is recommended that the day-night cycle match that of the natural levels the organisms would experience. While a simple binary on-off timer may be used to achieve this, it is better to include faders in the cosm facility design to gradually increase or decrease light levels over the course of the day as they would occur in nature.

Additionally, the potential for the turbulence-generation apparatus in a cosm to shade the water below should be considered. Placing grids, paddles, impellors and similar structures into a tank can decrease the amount of surficial light that reaches the bottom of cosm. This was considered to be an issue in a study by Rijkeboer et al. (1990), who promptly replaced a steel paddle with a transparent Perspex one to minimise this effect.

Temperature and salinity

As with light levels, it is also prudent to expose test organisms to temperatures and salinities that they would ordinarily be subject to in natural aquatic environments. While temperature has the ability to directly alter photosynthetic and respiration rates in

phytoplankton (Staehr and Sand-Jensen, 2006), there are also indirect temperature effects including variations in the solubility of gases. Both temperature and salinity have an influence on water viscosity which could affect microscale turbulence dynamics. In addition, temperature has been found to be inversely related to cell volume (Naselli-Flores et al., 2020), resulting in additional hydrodynamic variations that need to be considered.

Biological considerations

While smaller nano- and microcosm experiments lend themselves well to studying the effect of turbulence on a single species, larger mesocosms can be used to investigate interactions between two (or more) species (Havskum, 2003; Stoecker et al., 2006; Pannard et al., 2007; Fraisse et al., 2015; Martínez et al., 2017). Due to their apparent sensitivity to turbulence as well as their propensity to form harmful algal blooms, a majority of studies have understandably focussed on the dinoflagellate group (Figure 5). Furthermore, this group includes species with bioluminescent abilities; the light intensity emitted can be used as a proxy for turbulent shear, thereby facilitating the quantification of shear in cosm experiments (Stokes et al., 2004).

If using a natural planktonic population, it is possible to omit micro-zooplankton by filtering the water used prior to filling the cosms (Båmstedt and Larsson, 2018). While this is not suitable for predator-prey interaction studies, the removal of grazing should allow the subtle impacts of turbulence interactions on the phytoplankton community to be more easily observed. Choosing the correct filter to omit zooplankton grazers but not affect the larger size fraction of phytoplankton can be difficult due to the overlap in sizes of these groups. It is also likely that a natural phytoplankton population might contain mixotrophic ciliates and dinoflagellates that graze on other species.

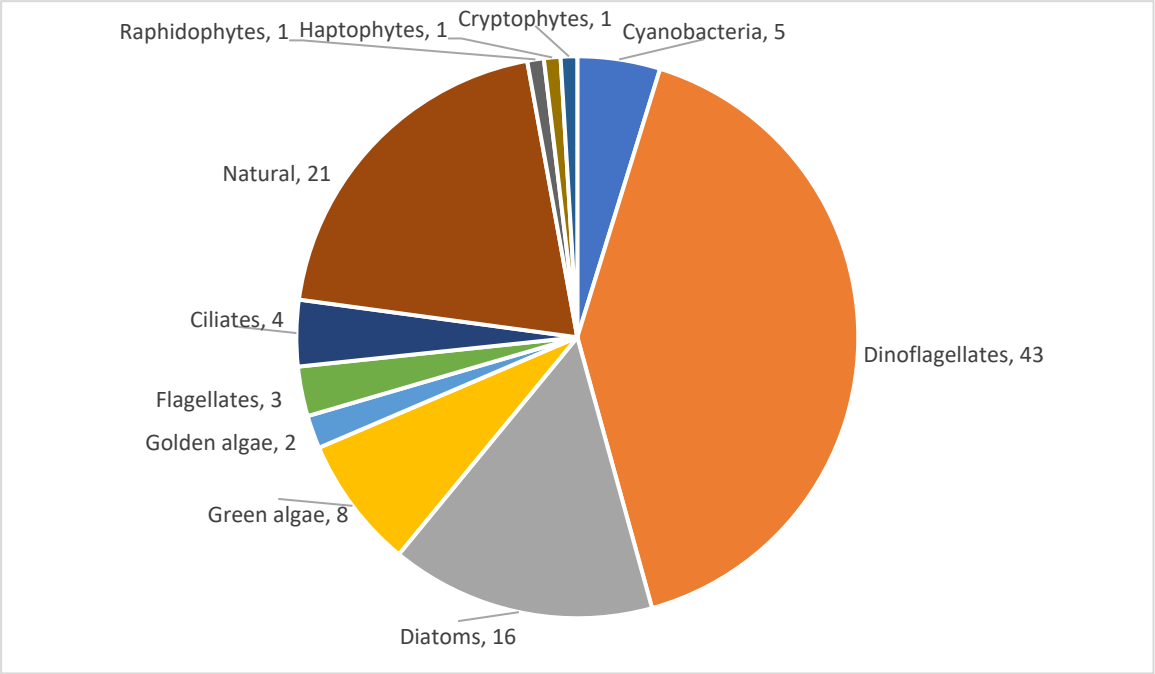

Figure 5 - Proportion of different phytoplanktonic groups used in the evaluated turbulence-interaction experimental studies. Number of publications featuring that group is included next to each segment. "Natural" refers to experiments that made use of indigenous populations.

METHODS OF TURBULENCE GENERATION

There are many ways to artificially generate turbulence in a laboratory environment; reviews of each of these different techniques and notable case studies for each are provided in this section. An analysis of previous methods identified that most studies use just four different methods: bubbling aeration, Couette cylinders, oscillating grids and laboratory shaker tables.

The chronology of publications (Figure 6) mirrors the information displayed in Table *1*; clearly grid-generated turbulence is the “industry favourite” with regards to phytoplankton-turbulence studies. Despite a boom in studies between 2000 and 2010, the recent decade has seen a decline of bio-turbulence publications; the lowest since the pre-1970s.

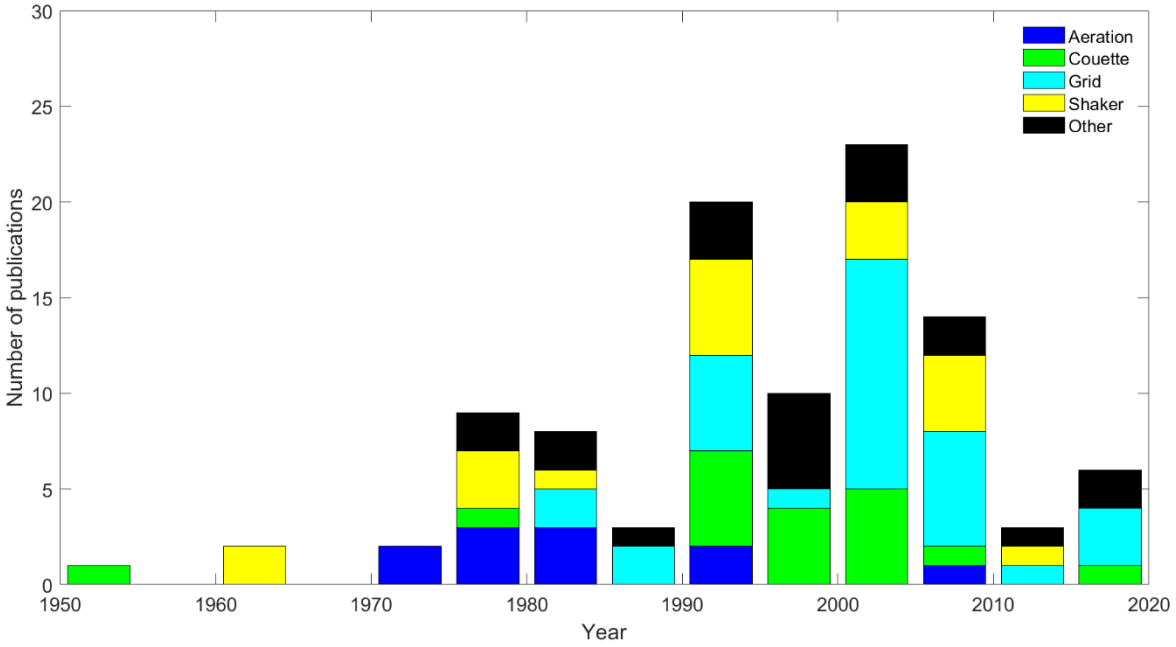

Figure 6 – Stacked bar chart of phytoplankton-turbulence publications by year showing the proportion of different turbulence-generation techniques used.

Oscillating grids

A standard way to generate turbulence within a tank is to use a grid mesh which is placed in the tank and connected to a mechanism that allows that grid to move through the water. This technique, referred to as "*a favourite in fluid dynamics experiments*" (Guadayol et al., 2009b) is often the preferred method of turbulence generation due to its simplicity as well as its established use in an extensive number of studies of this nature. Grids are typically of a similar width / diameter to the test tank and are a simple way to ensure a consistent turbulent field across the width of a tank. Typically, the grids are attached to a motor that allows them to oscillate vertically or horizontally at a given frequency and stroke length. A majority of these studies quantify ε (

Table *1*; Figure 6) whereas early experiments simply used motor settings or revolutions-per-minute (rpm) as a proxy for turbulence intensity.

As with the tank material, the grid itself can be made from any material but it is important that the grid does not corrode or deteriorate with time and remains biologically inert. For this reason, the use of ferrous metals is discouraged as these materials will not only degrade in saline water but will also provide a source of iron micro-nutrients. Netlon meshes are typically used as they come in a variety of mesh-sizes and are hardwearing, easily available, and corrosion-resistant. It is also possible to coat metal grids in inert substances such as nylon (Savidge, 1981).

In a thorough comparison between turbulence generated by grids to orbital shakers, Guadayol et al. (2009b) measured turbulence generated in a variety of different sized vessels ranging from small 0.8 L nanocosms up to 2500 L microcosms. As well as tank size, different grid configurations were trialled with variations in mesh size, bar width, grid diameter and cross-sectional shape. Study results show that the turbulence generated using grids was surprisingly isotropic (especially given the array of tanks size, grid dimensions and oscillation speeds) but with the caveat that grid stroke length had to be comparable to the depth of the tank. As such, Guadayol et al. (2009b) recommended using the maximum stroke length possible in order to ensure isotropy.

Vertically oscillating grids

In order to mimic surface layer mixing, grids are typically suspended from the top of the test tank. Grid nets can be singular (Savidge, 1981) or suspended in series of two or more grids (Estrada et al., 1987; Alcaraz et al., 1988; Berdalet, 1992). There is also the option of suspending an inclined, rotating ellipsoidal grid at a specific depth to promote mixing horizontally as well as vertically (Estrada et al., 1987). While investigating an alternative method to using grids, a number of disadvantages to using grid systems were identified by Webster et al. (2004). Having an object moving through the study tank interferes with many

direct flow measurement techniques; however indirect techniques, such as particle tracking velocimetry, can be readily used. Moving grids can also increase the likelihood of mechanical damage to the study organism. In studies where the grid oscillates in only a small fraction of the cosm, the turbulence field produced is non-isotropic and directional in accordance with the direction of the grid motion. In this instance, the turbulence generated is also heterogeneous as it decays with increasing distance from the grid. Webster et al. (2004) also cited size, expense and complexity of apparatus as major disadvantages of grid systems; in reality, however, a simple oscillating grid is vastly simpler than many other turbulence-generation methods described herein. Furthermore, Warnaars et al. (2006) recognised that steep turbulence gradients are typically recorded with grid systems; ε is highest near the grid but decays rapidly with distance from the grid. In addition, ancillary flows are seen to accompany the primary flow field which exposes any test organisms to a wider range of turbulent regimes than may be desired. Overall, Peters and Redondo (1997) discouraged the use of oscillating grids on the grounds that the turbulence produced is not properly representative of naturally occurring turbulence.

One disadvantage of grid systems is the steep turbulence gradients found around the grid itself. If test organisms are permitted in and around the oscillating grid, they not only risk mechanical destruction but are also exposed to a wider range of ε than they would in a natural environment. To prevent organisms from interacting with the region of grid oscillation, MacKenzie and Kiørboe (1995) used a fine mesh placed below the grid. The study focussed on swimming behaviour and encounter rates between copepod larvae and cod / herring larvae; thus, the barrier mesh size was selected to allow the prey copepods to interact with the grid region while the fish larvae were unable to enter this region. The addition of the mesh screen is a notable improvement to studies of this nature but could interfere with the turbulent field produced by the oscillating grid. There is also the possibility that prey could pass through the

mesh screen where it could then be subjected to advantageous conditions for increased growth. The presence of the screen could then prevent the now larger organism from passing back through the mesh. In the case of phytoplanktonic studies with incident light from above, this could provide an intrinsic bias to the study.

Horizontally oscillating grids

While most practitioners opt for vertically oscillating systems, there are times when a horizontal system is more suitable. To reduce the likelihood of resuspension of filamentous and dense species that sediment to the bottom, horizontal grids are better suited if using a mixed phytoplankton community as shown in a study by Fraisse et al. (2015). Six different phytoplankton species were selected to represent an array of morphologies (elongated shapes, flattened shapes and motile species), densities, growth rates and sizes. The study showed that the species selected that had high sinking rates were unable to outcompete those that could maintain their positions in the upper column. Similarly, Schapira et al. (2006) made use of horizontal grid systems taking care to produce both realistic and quantified turbulence measurements. Opting for low, medium and upper limits of turbulence found in the English Channel, the researchers investigated the impact of this on the colony-forming dinoflagellate *Phaeocystis globosa* Scherffel. Results show that turbulence enhanced colony growth and formation to a threshold amount after which turbulence was found to impede cell growth via a postulated reduction in cell division (Schapira et al., 2006).

Vibrating grids

In addition to oscillating grids, vibrating grids have also been used; to study the effects of turbulence on zooplankton behaviour, Saiz and Alcaraz (1992) utilised a vertically orientated grid attached to a vibrating rod which moved the grid in the horizontal axes (x and

y). Efforts were made to not only quantify the turbulence generated but to also map the turbulence field across the tank; it was found that the vertical and horizontal components of ε did not differ to any significant extent. The results of the experiment showed that the increase in turbulence caused a corresponding increase in both copepod suspension and predatory feeding behaviour thought to result from an increase in predator-prey contact rates (Saiz and Alcaraz, 1992).

Stationary grids

Looking to improve the often-used grid oscillation systems, Warnaars et al. (2006) used a pair of underwater speakers in anti-phase to push water through a stationary grid placed directly in front of each speaker. It was observed that the flow characteristic of the speaker system compared well with grid systems, albeit with lower strain rates making it more representative of natural turbulence fields. Furthermore, ε is seen to attenuate rapidly with distance from grids in oscillator set-ups; however, the speaker system generated uniformly distributed ε throughout the entire volume of the tank. It is also noted that the range of turbulence scales observed in grid systems is larger than those measured in the speaker system; when the chlorophyte *Selenastrum capricornutum* Printz was exposed to the speaker system, growth rate was seen to increase as conditions became more turbulent. This increase in growth was attributed to the fact that the range of ε experienced by the organisms is more concurrent with the levels in the natural environment. It should also be noted that in the absence of a moving grid, this technique permits direct flow velocity measurements. Due to limitations imposed by equipment practicalities, however, this technique would likely be restricted to nanocosm and microcosm experiments.

Additional case studies

A number of researchers have used similar grid-generated turbulence set-ups to observe predator-prey interactions within turbulent environments (Peters and Gross, 1994; Peters et al., 2002; Dolan et al., 2003; Havskum, 2003; Havskum et al., 2005). For example, Havskum (2003) investigated how grid-generated turbulence affected feeding rates of a predatory dinoflagellate species linking turbulence to the rate of predator-prey interaction. The disadvantage of studies of this nature is that, as well as altering the encounter rate, in many cases the turbulence causes secondary physiological or behavioural changes in the species studied (e.g., Peters and Gross (1994)). When conducting cosm experiments of this nature, it is crucial to use planktonic species that are not sensitive to turbulence; for example, Havskum et al. (2005) observed no change in the autotrophic or mixotrophic growth of the dinoflagellate *Fragilidium subglobosum* (Stosch) Loeblich III under different turbulence levels but did observe a change in ingestion rates.

In a technique analogous to grid-generated turbulence, Sullivan and Swift (2003) used a pair of vertically oscillating rods to produce varied intensities of turbulence. Interestingly, this paper opposed the commonly held view that dinoflagellates as a group are sensitive to turbulence; out of the 10 species tested, 7 were unaffected by natural levels of turbulence. In a similar departure from vertically oscillating grids, researchers at the Marine Ecosystem Research Laboratory (MERL; Rhode Island, USA) mesocosms made use of a rubberised plunger attached to a vertical pole to simulate tidal mixing. The plunger itself was situated 1m above the sediment-laden floor to provide realistic levels of tidal sediment resuspension with the system motor timed to providing a mixing cycle mirroring natural tidal oscillations (Santschi, 1985).

Towards the larger scale of mesocosm studies, it is also possible to use grid-generated turbulence in limnocorrals (Nerheim et al., 2002). Studies undertaken as part of the Nutrients

643 and Pelagic Production project (Nejstgaard et al., 2001b; Nejstgaard et al., 2001a; Nerheim et
644 al., 2002) encountered difficulties with this approach, however. In order to promote
645 stratification in some of the limnocorrals, freshwater was added to the surface; this resulted in
646 the limnocorrals rising up out of the water as the mean internal water density was now lower
647 than that of the surrounding water. This effect was countered by increasing densities via the
648 addition of salt to the water in the lower parts of the mesocosms. Altering the salinity to this
649 extent in a biological study is not advised as this would alter the phytoplankton community in
650 favour of species that are less sensitive to changes in salinity. Once stratification was
651 established in the NAPP studies, the grid mixing systems were then used to promote an upper
652 mixed layer while a low-suction airlift pump system (typically used in aquaculture or marine
653 archaeology) promoted "slow circulation" in the upper layer.
654
655 **Shaker tables**
656 Shaker systems are used across a multitude of sciences for a variety of applications
657 from agitation of chemicals to the culturing of microbiological organisms. Due to the ubiquity
658 of shaker tables in academic and scientific institutions, it is not unsurprising that they are
659 frequently used to generate artificial turbulence. Furthermore, they typically have discrete
660 settings allowing researchers to generate a broad range of turbulence levels. While some
661 researchers simply use the rpm settings, more rigorous studies quantify the level of turbulence
662 via acoustic Doppler velocimetry or similar. It should be noted that specific turbulence flow
663 patterns generated by shaker tables are difficult to quantify, thus any recorded changes in
664 biological activity is difficult to ascribe to a particular flow characteristic (Warnaars et al.,
665 2006). Shaker tables typically use one of three different motion paths depending on their
666 intended application: orbital or rotary shakers; reciprocal shakers; and, gyratory shakers
667 (Figure 7).

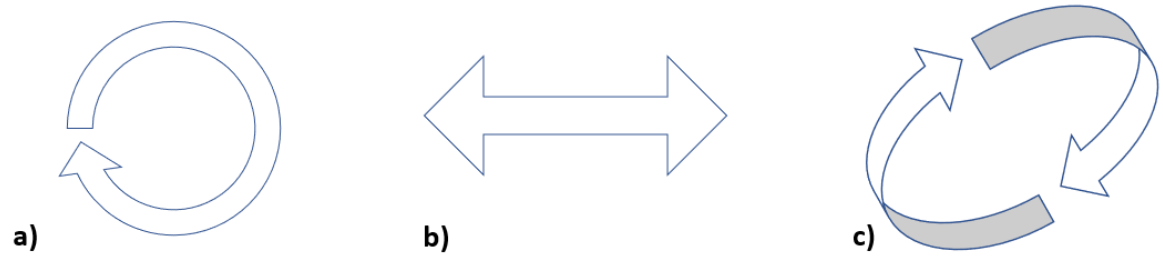

Figure 7 - Motion paths of vessels placed on different types of shaker tables as seen from above. a) An orbital / rotary shaker oscillates in a circular motion in the x-y plane. b) A reciprocal shaker oscillates from side to side along a single axis. c) A gyratory shaker oscillates vessels in a circular motion with both horizontal and vertical components to the motion.

Orbital shakers

Orbital shakers (a.k.a. rotary shakers) agitate cultures with a circular motion in the x-y plane (Figure 7a). Depending on the manufacturer of the shaker, the orbit oscillation is fixed at a set distance or can be altered accordingly. Zirbel et al. (2000) used orbital shakers to observe changes in dinoflagellate morphology over time. Trials were conducted with the shakers set on 40 rpm to 120 rpm before a rate of 75 rpm was designated as "*relatively mild*" turbulence. It is noted that for such shaker experiments, turbulence occurs due to wall effects within the vessel. This has two ramifications: firstly, the turbulence will increase with proximity to the vessel walls and secondly, the vessel needs to be of a suitable size to allow turbulent mixing to impact upon fluid in the centre (Peters and Redondo, 1997). Orbital shakers typically promote the central "doldrum," or dead-space, region in flasks marked by minimal in situ turbulence meaning that the cells are no longer being cultivated under near-isotropic conditions (Juhl et al., 2000). Furthermore, the turbulent mixing produced would be predominantly horizontal with a weak secondary vertical component. However, horizontal eddy diffusivity in the ocean is thought to be "*several orders of magnitude*" greater than the vertical equivalent (Okubo (1976) cited in Estrada et al. (1987)).

As shaker table experiments typically make use of available apparatus, there is often a range of different sized and shaped vessels used which makes comparisons between studies difficult. In a comparative study between turbulence generated by grids versus that generated by orbital shakers, Guadayol et al. (2009b) trialled a number of different shaker set-ups with different periods of oscillations as well as various volumes and flask (Florence, Nalgene and Erlenmeyer) types. The research showed that at high levels of shaking, the turbulence field remains isotropic independent of volume or flask shape. However, at lower levels of ε ($< 10^{-8}$ m^2/s^3), the isotropy began to fall, probably as a result of lower signal-to-noise ratios (SNR) in the Doppler velocimeter as well as the fluid approaching the laminar-turbulent transition point. Furthermore, orbital frequencies of <1 Hz are not recommended as it at approximately this frequency that the laminar-turbulent transition occurs in flasks. As orbital shaker turbulence is generated via wall friction, ε decreases with distance from the sides and bottom; an order of magnitude decrease in ε was observed in measurements when transitioning from the wall to the centre of the flask. Thus, it is recommended that "*small and narrow*" vessels (e.g. Nalgene flasks) be used to limit this effect as much as possible (Guadayol et al., 2009b).

Reciprocal shakers

Reciprocal shakers oscillate from side to side along a single axis in the x- or y-plane (Figure 7b). The length along which the oscillation occurs can be altered accordingly with longer lengths equating to higher levels of turbulence (Juhl et al., 2000). The advantage of reciprocal shakers is the removal of the central doldrum in the flasks which typically occurs in orbital shakers. In a comparative study of the effects of shaker-table-generated mixing relative to Couette-generated shear flow, Juhl et al. (2000) subjected populations of the dinoflagellate *Lingulodinium polyedra* (F. Stein) J.D. Dodge to different durations of constant mixing. Actually, reciprocal tables allow standing waves to form in the flask, resulting in an

oscillating fluid surface that ensures all cells in the population experience variable mixing. While the level of turbulence was not quantified directly, attempts were made to approximate mixing via a comparison of the qualitative outcome between the shaker populations and the Couette populations; the response of the cells exhibited a similar response in both setups.

Gyratory shakers

As well as orbital shakers and reciprocal shakers, there are also gyratory shakers which oscillate vessels in a circular motion with both horizontal and vertical components to the motion (Figure 7c). An experiment was carried out to observe effects of gyratory-shaker-generated turbulence (as well as of growth medium, fluid depth, tank material and initial cell concentration) on the doubling time of the protozoan *Tetrahymena* sp. (Hellung-Larsen and Lyhne, 1992). It was noted that gyrational shaking resulted in a circular wave that propagated around the edge of the shaking vessel. The study showed that the doubling time was increased (i.e., cell division decreased) with shaking but the impact of the shaking reduced with increased fluid depth. Morphologically, cells that were exposed to shaking exhibited less-prominent nuclear membranes and the development of small granules inside the cell cytoplasm. It was also observed that viscosity played a role as the effect of shaking on cell division was reduced when dextrane was added to increase the viscosity of the medium; clearly, the increase in viscosity acted to reduce the overall level of turbulence in the vessels. The study also compared the impact of gyratory agitation to reciprocal shaking and bubbling; when using gyrational shaking, the impact of shaking rate on cell division was seen to be dependent on initial cell concentration, but this was not so for reciprocal shakers (Hellung-Larsen and Lyhne, 1992).

Additional case studies

Building upon early work regarding the mass culture of algae, Fogg and Than-Tun (1960) used a shaker apparatus to ascertain the optimum shaking speed to maximise cultures of *Anabaena cylindrica* Lemmermann. Even low agitation speeds were seen to increase cell growth compared to unshaken cultures. While moderate shaking was seen to increase growth due to increased suspension and nutrient flux, if the shaking rate exceeded 140 rpm, the cell growth rate showed no increase when compared to unshaken cultures. Opposing these findings, Tuttle and Loeblich (1975) attempted to find the optimal growth conditions for the dinoflagellate *Crypthecodinium cohnii* (Seligo) Chatton and observed exponential death rates of cells at both 40 and 80 rpm; these early results hinted at the turbulence sensitivity of some dinoflagellate species.

In what has now become a classic paper in the study of phytoplankton-turbulence interaction, White (1976) used rotary shakers to agitate cultures of *Alexandrium tamarense* (Lebour) Balech to note the effect on cell growth while investigating the cause of red tides in Eastern Canada. Results show that cell growth reduced rapidly at high levels of continuous shaking; even intermittent shaking and/or shaking at low speeds was seen to adversely affect cell growth. As well as mechanical destruction, White (1976) attributed the decreased growth rate to cell disorientation that caused subsequent interference with phototactic migration. Peters and Marrasé (2000) have since estimated the turbulence generated in this study to be higher than natural ε with values between 4.30×10^{-3} and 1.19×10^{-2} m^2/s^3. While the White (1976) study made no attempt at turbulence quantification (it was, after all, at the time seen as a purely biological study), it none-the-less sparked interest in turbulence studies within the marine ecological community.

Clearly drawing upon these findings, Berdalet (1992) sought to identify the mechanism(s) by which cell growth is reduced in turbulence. Cultures of the HAB

766 dinoflagellate *Akashiwo sanguinea* (K. Hirasaka) Gert Hansen & Moestrup were exposed to
767 shaker-table turbulence with cellular volume, shape and location of nuclei, RNA and DNA
768 concentrations all recorded. Berdalet (1992) postulated that the observed reduction in growth
769 was a result of the physical disruption of chromosome separation during cell division. Again ε
770 was unquantified in this study (Peters and Marrasé (2000) later estimated the corresponding ε
771 as 2 x 10^{-3} m^2/s^3), but more recent studies based on the same experimental set-up utilised an
772 acoustic Doppler velocimeter to record water speed at different points in the flask (Berdalet et
773 al., 2007). Of relevance within the current review is a thorough literature overview of all
774 experiments on turbulence-dinoflagellate interactions which, as per Peters and Marrasé
775 (2000), includes estimates for ε calculated using experimental set-up data from individual
776 experiments (see Appendix 3).
777
778 **Aeration systems**
779 When biologists look to cultivate cells, they often seek to aerate the water via a bubble
780 stone at the base of the tank which allows gases (e.g., CO_2, oxygen) to diffuse into the water,
781 promoting growth. As such, bubble plumes and aeration systems in the lab are a tried and
782 tested technique for mixing water and aerating growth tanks. Furthermore, most
783 microbiological laboratories have access to air compressors and piping to facilitate the use of
784 aeration systems. A by-product of this aeration is that the bubbles themselves break down any
785 stratification, thereby homogenising the water while also advecting the cells as the central
786 bubble plume effectively promotes formation of a toroidal convection cell in the tank. Within
787 the mesocosm community, aeration systems are typically seen to be gentler in their approach
788 to turbulence generation due to their absence of moving parts that have the potential to
789 mechanically damage organisms (Sanford, 1997; Striebel et al., 2013).

In laboratory setups, it can be difficult to determine whether the change in growth rate is a result of the turbulence induced by the bubble flow or as a result of atmospheric gases being entrained through the water. How the culture will react is species-dependent with dissolved oxygen being required for respiration while CO_2 promotes photosynthesis. Gas addition can also result in a change in pH via CO_2-induced decreases in the pH of water; this can have impacts for pH-sensitive species (Havskum and Hansen, 2006). An unintended side-effect of bubbler aeration systems is a temperature change to the fluid medium. As gases that are introduced to the fluid are typically at air temperature, this can impart additional thermal energy to the system. Furthermore, as the gas has typically undergone pressurisation prior to release, there may also be associated adiabatic thermal effects.

Båmstedt and Larsson (2018) noticed an aggregation of bacteria, algae and detritus at the water surface of their unmixed cosms during experiments. This was thought to be the result of surface heating from the overhead irradiance lamps causing a thermal lid effect in the upper 60 cm. It was found that bubbling at a rate of 1 Hz from 2 cm depth was sufficient to break up the surface aggregation, but some mixing was required to break the thermal lid. As such, a comparison between bubbling and surface mixing using fans angled at 45° to the surface was carried out; overall fan mixing was found to mix the mesocosm faster than bubbling. It should be taken into consideration that the bubbler system was set to emit a single 18 mm-diameter bubble at 1 Hz so as to not cause any undesirable aeration effects.

In an attempt to determine the optimal conditions for cultivating the dinoflagellate *Crypthecodinium cohnii*, Tuttle and Loeblich (1975) subjected cultures of cells to agitation by aeration (as well as magnetic stirrers and shaker tables). Sterilized air was bubbled through the medium at a rate of 1.8 L/min; the increase in observed growth rate was negligible. In a series of experiments exploring potential biomass species, Thomas et al. (1984a); Thomas et al. (1984b); Thomas et al. (1984c) used aeration systems to “vigorously” aerate and mix the

cell cultures. Using a gas mix of 1% CO_2 in air, two aeration pipes were placed at the bottom of the tank and gas supplied at a rate of 2000 ml/min. The researchers reported "very high densities" and reported no evidence of mechanical damaging of the cells despite the high aeration rate. There was no control tank setup nor any attempt to quantify the turbulence produced. Again, with reference to the commercial cultivation of phytoplankton, Aguilera et al. (1994) used bubbler agitation in chemostats to mix cultures of a microalga. Novel in this experiment was an attempt to quantify mixing in terms of mechanical energy supplied to the system calculated using standard physical equations relating gas pressure, velocity, and the conservation of mass and/or energy. Within this work, the role of turbulence was recognised in preventing sedimentation, promoting a homogenous distribution of cells and nutrients, and increasing the nutrient supply to the surface of the cell. However, agitation by bubbles was also cited as a way by which gases are more efficiently diffused into the medium. As discussed earlier, this effect of increased gas diffusion on cell growth would be difficult to distinguish from changes due to the increase in turbulence.

Aeration systems have been used to good effect for studying natural planktonic communities (Eppley et al., 1978; Sonntag and Parsons, 1979). As part of the Controlled Ecosystem Pollution Experiment (CEPEX), Sonntag and Parsons (1979) used aeration to simulate upwelling, then added salmonids to create an additional trophic layer that would ordinarily be absent (the enclosures were taken to depth by divers and then slowly raised so any suitably motile organism would have been able to escape). The study recorded high rates of phytoplankton sedimentation suggesting that the aeration regime chosen was insufficient to promote resuspension. Using the same limnocorrals, Nerheim et al. (2002) combined grid-generated turbulence with an aeration system to study a natural food web. Researchers quantified the rate of vertical mixing via a dye dispersion study; this led them to realise that the vertical eddy diffusivity was 0.06 cm^2/s, lower than the expected value outside of the

enclosures (Steele et al., 1977). It was thus postulated that the presence of the enclosures reduced the horizontal mixing and as this is coupled to vertical mixing, there was a subsequent impact on vertical mixing also. Efforts were made to limit daily mixing to the level just required to break any measured stratification; however, no efforts were made to quantify this vertical mixing. Microscopic analysis of the species within the enclosures verified that the bubbles did not damage cells mechanically, with Eppley et al. (1978) reporting "no grossly unnatural results".

Couette cylinders

Named after French physicist Maurice Couette who first used them in 1890 (Couette, 1890), this equipment generates shear flow in a small gap between two concentric cylinders. A fluid medium is placed in the gap between the smaller inner cylinder and the larger outer cylinder. The inner cylinder then rotates at a given speed producing uniform flow conditions (Peters and Redondo, 1997; Sullivan and Swift, 2003). A key advantage of this setup is that shear flow can be easily calculated from angular velocity, thereby removing the need for physical measurements to calculate flow parameters. Furthermore, a variety of different forms of turbulence can be produced by rotating the cylinders at different velocities relative to each other. However, Sullivan and Swift (2003) reported that the turbulence produced by Couette cylinders is intrinsically unrepresentative of natural turbulence because it applies constant shear both temporally and spatially.

Some of the first phytoplankton-turbulence studies were carried out using Couette cylinders. Pasciak and Gavis (1975) conducted a series of experiments on the effect of turbulence on nutrient uptake rate in diatoms. Interestingly, they compared the uptake rate between cell cultures on orbital shaker tables to those inside a Couette flow. While the shear flow rate was calculated for the Couette flow, no attempt was made to quantify the turbulence

865 generated inside the flasks on the shaker table. Building upon this work, Thomas and Gibson
866 (1990a,b) used an almost identical set-up to observe the impact of shear flow on nutrient
867 uptake on *Lingulodinium polyedra*, a HAB-forming dinoflagellate species. Using a series of
868 Couette cylinders with rotational speeds ranging from 1 rpm up to 60 rpm, the researchers
869 calculated various turbulent parameters using the rotational speed.
870 Using a similar Couette set-up, Juhl et al. (2000) also conducted an investigation on
871 the dinoflagellate, *Lingulodinium polyedra*. The aim of this experiment was to account for the
872 variability in studies by measuring the effect of turbulence on population growth under
873 varying light-dark cycles, differing light levels and different stages of the cell cycle. The
874 outcomes highlighted a number of key mechanisms: a) that cell growth rate decreased more
875 when flow was applied in the last hour of the dark phase as compared to applying it to
876 illuminated cultures; b) populations cultured in lower light conditions experienced
877 proportionately lower growth rates when exposed to flow than those cultured in higher light
878 conditions and c) older cultures in the late exponential phase experience higher mortality
879 under flow than cells in the early phase. A key outcome of this study was that the extent to
880 which turbulence affects the cell population is not only light-dependent but also depends on
881 the physiological state of the cell (and the phase of its life cycle).
882 Juhl et al. (2000) also compared the outcomes of the Couette studies to equivalents carried out
883 using turbulence generated using shaker tables. Unfortunately, the shaker table turbulence
884 was unquantified; however, attempts were made to approximate the shear flow via a
885 qualitative comparison of results. It should be noted that Warnaars et al. (2006) recognised
886 that the minimum strain rate used in the studies of Thomas and Gibson (1990a,b) were up to
887 two orders of magnitude greater than those observed in the natural environment.
888

889 A summary of turbulence generation methods and associated advantages and
890 disadvantages can be found in Table 3, along with example references highlighting best
891 practice for each of the main techniques. Based on this review, it is recommended that
892 oscillating grids become the turbulence-generation standard; of the techniques evaluated, the
893 grid-generated turbulence is closest to that found in natural systems. Furthermore, it is
894 relatively easy to adjust the experimental set-up in order to facilitate species across different
895 groups and, on a broader topic scale, across the different marine science sub-disciplines. This
896 technique is also the most commonly used (
897 Table *1*), thereby facilitating easy comparisons with any future study. See Appendix 1
898 for a summary of lesser-used techniques for generating turbulence including pumping,
899 magnetic stirrers, rotating chambers, wave tanks, impellors / propellers, paddles, dialysis
900 cylinders and convective mixing.
901
902 *Table 3 - Summary table of commonly used turbulence generation techniques*

Technique	Pro	Con	Example
Oscillating Grids	• Can be configured for near-isotropic turbulence • Reduction in resuspension (horizontal grids) • Can use mesh screens to create refuge area	• Obstructs flow velocity measurement equipment • Risk of mechanical damage to organisms • Steep turbulence gradients; ε highest near grid but decays rapidly with distance	Schapira et al. (2006)
Shaker tables	• Low-cost, off-the-shelf equipment • Commonly found in laboratories	• Typically restricted to small volumes • Turbulence generated is non-isotropic with high ε near flask wall decreasing towards centre	Berdalet et al. (2007)
Aeration systems	• Can be applied across all scales of cosm • Commonly found in microbiological laboratories	• Introduction of gases causing secondary growth effects in cells • Bubbles can cause adiabatic thermal effects and impede flow velocity measurements	Aguilera et al. (1994)

	• Possible to use equations to estimate turbulence from energy input	• Not quantifiable turbulence	
Couette cylinders	• Shear flow can be calculated from angular velocity, removing the need for physical measurements	• Turbulence unrepresentative of natural systems	Stoecker et al. (2006)

903

904

METHODS FOR QUANTIFYING TURBULENCE

It is crucial to properly describe the nature and quantify the magnitude of the turbulent environment within a cosm. To relate a cosm experiment back to its intended real-world application, organisms should be exposed to turbulence that mirrors natural turbulence as closely as possible. While some studies simply use the rate of motor revolutions as a proxy for turbulence quantification, others use an array of techniques to maintain turbulence requirements. It should be noted that a majority of turbulence-generation techniques involve the placement of movement apparatus in the test tanks (e.g., grids); as a result, it becomes difficult to place sensors for turbulence measurement undisturbed in the tank as well.

Instead of measuring turbulence directly, some researchers simply consider the mechanical energy input to the cosm (Kiørboe et al., 1990; Aguilera et al., 1994; Martínez et al., 2017). For example, in a grid-generated turbulence study, Kiørboe et al. (1990) was able to calculate ε as a function of power input from the motor as $\varepsilon = W/V \times 1/\rho$, where W = power input (W), V = volume of fluid (m^3) and ρ = density of fluid (kg/m^3). While easily calculated, these values are often theoretical and can be presented without proper calibration. Given the ad hoc nature of many turbulence experiments, this estimate of ε (and associated calibration) must be considered on a case-by-case basis (Guadayol et al., 2009b). Furthermore, it also makes comparison between different studies difficult as this ε value is not standardised nor easily comparable to natural systems.

The following section provides an overview to the various techniques used to quantify turbulence as well as any corresponding advantages and/or disadvantages. Methods reviewed include particle tracking velocimetry, particle imaging velocimetry, planar laser induced fluorescence, Doppler velocimetry, and calculation via empirical formulae. Figure 8 shows a breakdown of how frequently various methods have been used for turbulence quantification.

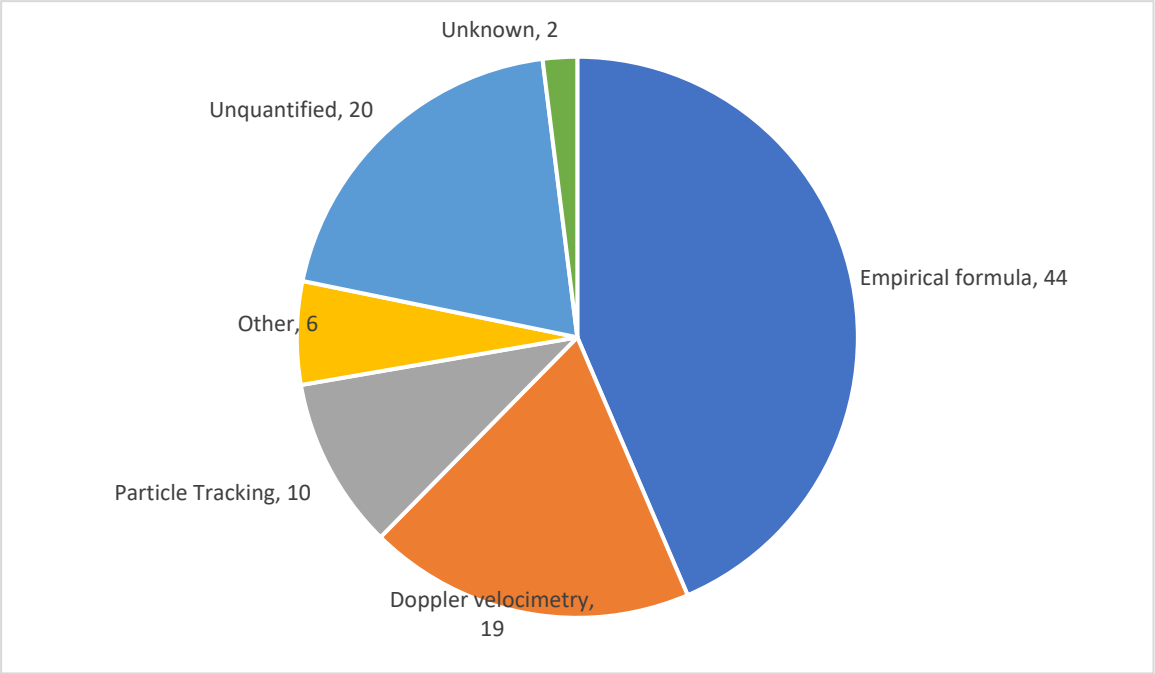

Figure 8 – Methods used to quantify turbulence in the publications reviewed. Particle tracking: refers to particle tracking velocimetry, DPIV and PLIF. Doppler velocimetry: refers to ADV and LDV. Other: refers to dye dispersion and bioluminescence.

Particle tracking velocimetry

As a precursor to digital image analysis techniques, early particle imaging was carried out using video recorders attached to microscopes (e.g. Saiz and Alcaraz (1992)). This technique involves the direct imaging of individual tracer particles (e.g., reflective spheres or phytoplankton cells) highlighted by a sheet of laser light. An image is taken and compared to another image taken some small time period later. The subsequent direct image comparison allows for local particle displacement to be determined. By accounting for the time delay and image magnification, it is possible to map the velocity field of a tank. While this analysis has proven to be computationally expensive, it does result in a high vector density with good accuracy and spatial resolution (Webster et al., 2001). The image field is then divided into a grid, the instantaneous velocities are decomposed into horizontal and vertical components, the spatial means within a grid cell are computed. This spatial mean is then subtracted from the instantaneous velocity field to yield the fluctuating component of the particle velocities,

948 which is representative of the turbulence in the flow, and, from this, the turbulent dissipation
949 rate can be determined (Marrasé et al., 1990; Saiz and Alcaraz, 1992).
950 Technological advances in velocimetry are now permitting fluid dynamicists to
951 measure the flow fields across illuminated planes within a cosm. As water is a transparent
952 medium, these techniques typically involve the illumination of particles suspended in the
953 fluid, as suspended sediment, planktonic organisms or artificially introduced reflective
954 particles. These particle tracking velocimetry techniques typically involve an external source
955 of illumination (e.g., a light or laser) and an external camera. Thus, a benefit of these
956 techniques is that they do not require apparatus to be placed in the test tank; hence, they can
957 be used with a variety of turbulence-generation methods. While advances in particle tracking
958 velocimetry now permit detailed imaging of 3D flows (Hoyer et al., 2005; Raffel et al., 2018),
959 this has yet to be applied to any bio-turbulence studies which, to date, have not progressed
960 beyond two-dimensional (2D) imaging. This technique is sometimes referred to as digital
961 particle tracking velocimetry (DPTV) (Webster et al. (2001).
962
963 **Digital Particle Imaging Velocimetry**
964 Digital particle imaging velocimetry (Digital PIV or DPIV) involves seeding the test
965 fluid with highly reflective neutrally buoyant particles. The size of the particles required is
966 dependent on the size of the fluid structures required by the study. A laser light sheet is then
967 projected into the tank resulting in an illuminated plane. This laser is synchronised to a digital
968 camera positioned perpendicular to the illuminated plane which photographs the particle
969 movement; this allows a velocity map of fluid motion to be produced. It is important to select
970 a suitable laser pulse and shutter speed to prevent signal distortion and other artefacts (Zirbel
971 et al., 2000). Older DPIV systems required the simultaneous use of two digital camera and
972 corresponding laser sheets to image 3D flow; this required unimpeded access to different

973 sides of the cosm (Eder et al., 2001). Fortunately, more modern techniques (e.g., tomographic
974 PIV; tomo-PIV) have streamlined the measurement of 3D and time-resolved (four-
975 dimensional) flows with both overall precision and higher spatial resolution (Scarano, 2012;
976 Raffel et al., 2018). Calculation of ε using PIV can be a mathematically complex procedure.
977 Assuming the turbulence is both isotropic and homogeneous, Xu and Chen (2013) simplify
978 the estimation of ε:

979 $$\varepsilon = 15\nu\left\langle\left(\frac{\partial u'}{\partial x}\right)^2\right\rangle \qquad (1)$$

980 where $\langle \cdot \rangle$ denotes a mean average, ν = kinematic viscosity (m^2/s), and u' = velocity
981 fluctuations in the x direction with $u' \equiv u - \langle u \rangle$ and u being the x-component velocity (m/s).
982 The introduction of lights and lasers into the fluid medium does have the potential to
983 influence the behaviour of the test organisms. Phototaxic phytoplankton species that use light
984 to orientate their swimming direction could be drawn towards the laser light. Furthermore,
985 high-intensity lasers could in theory cause photo-inhibition in photosynthetic organisms and
986 reduce the rate of primary production. Motile phototactic species could also be influenced;
987 however, Linares (2015) observed in a turbulence experiment designed to specifically study
988 the potential for laser-induced photoinhibition, that "laser exposure has little effect on
989 phytoplankton".
990 While it is standard practice to add tracer particles to the test medium to increase the
991 SNR (Estrada et al., 1987; Fraisse et al., 2015), it is important to select an appropriate tracer.
992 The motion of any tracer is assumed to follow the flow dynamics of a setup; the extent to
993 which the tracer particles accurately follow the flow can be determined via the Stokes
994 number. The test tracer should have a Stokes number << 1 in order for the tracers to mirror
995 the fluid movement; a Stokes number < 0.1 will ensure an accuracy of 99% (Tropea and
996 Yarin, 2007). A tracer should also be neutrally buoyant and sized appropriately; a smaller

diameter is preferable but should be large enough to be recorded. The tracer selected should be reflective so as to scatter the incident laser light; Webster et al. (2001) reported titanium dioxide particles have a superior reflectance to comparably sized nylon bead tracers or kaolin. Organic substances such as *Licopodium* pollen grains (Saiz and Kiørboe, 1995) and rheostatic fluid (made from fish scales (Latz et al., 1994; Hondzo et al., 1997) can also be used as tracers, though the addition of extra organic matter and its subsequent decomposition could influence growth rates. As such, tracers are normally added to cosms absent of test organisms. If a tracer is added to a tank containing organisms, it should be both non-toxic and non-influential on growth rates. For environmental reasons, it is prudent to avoid the use of microplastics; if the chosen tracer is a plastic, the particles should be recovered before disposal.

Planar Laser Induced Fluorescence

PLIF is similar to DPIV but makes specific use of the fluorescent properties of phytoplankton. As with DPIV, a laser sheet is introduced into the fluid medium to illuminate a 2D cross-section with the cosm. Phytoplankton cells are seen to have inherent fluorescent properties due to the presence of chlorophyll compounds and other photosynthetic cellular organelles. As such, phytoplankton cells are known to exhibit a peak absorption wavelength of light at ~440 nm. Following absorption, the light is subsequently re-emitted as a lower energy photon at ~685 nm manifesting itself as fluorescence (Leeuw et al., 2013). It is possible to calibrate this fluorescence intensity to attain cell concentration as well as directly measure the velocities of individual cells akin to DPIV (Liu et al., 2017). Interestingly, as technology has progressed the robustness of PLIF systems has increased to the point where these systems can be deployed directly in the field, allowing researchers to obtain in situ measurements on fluorescent particle distributions (Franks and Jaffe, 2008). As an extension

of PLIF, 3D laser induced fluorescence (3D LIF) technology exists that is able to reconstruct a 3D frozen-field image of a fluid flow by scanning perpendicular to the 2D laser sheet (Crimaldi, 2008); to date, no evidence could be found of it being applied to bio-turbulence studies. Despite the differences in technology, quantification of turbulence based on DPIV and PLIF draws upon the same calculations.

Relying on fluorescence does mean that any other photo-active particles and/or chemicals in the fluid medium will obscure the fluorescent signature. In particular, the presence of CDOM can preferentially absorb certain light wavelengths and attenuate light transmission through the water. The fluorescence intensity from certain dyes are also dependent on the pH and temperature of the water (Crimaldi, 2008), so this should be corrected for to allow comparisons between studies. Also of note is the process of photobleaching by which the fluorescent intensity of a dye or phytoplankton cell diminishes over time with prolonged exposure to high-intensity light of certain wavelengths; selection of a suitable dye should prohibit these effects but dyes that are less susceptible to photobleaching are typically more costly (Crimaldi, 2008).

Doppler velocimetry

Doppler velocimetry involves introducing a soundwave or laser of known frequency into a fluid medium. This beam is then reflected off moving particles within the fluid causing a measurable frequency shift. Doppler velocimetry allows the user to accurately measure 3D mm-scale velocities within a water body.

Acoustic Doppler Velocimetry

Single-point velocity Acoustic Doppler Velocimeters (ADV) can be used to good effect to measure 3D point velocities. As the name would suggest, ADVs utilise the Doppler

1047 effect by which a pulse of sound of a known frequency is sent into the water from a central
1048 transducer. This pulse is reflected by particles in the water back to three receivers which
1049 calculate the motion of the water from the shifted frequency. The reflective particles in the
1050 water can be natural (e.g., sediment, microorganisms) or artificial (e.g., seeded particles in test
1051 tanks). The addition of such particles greatly improves the SNR, which is especially useful in
1052 quiescent flows.

1053 While the resolution of the instrument varies with manufacturer (as well as sampling
1054 rate and sampling volume), one can directly quantify different turbulence parameters with
1055 suitable processing by measuring Reynolds stresses (Lohrmann et al., 1995) or by fitting the
1056 Kolmogorov –5/3 slope to the inertial subrange of the velocity spectra (Bluteau et al., 2011).
1057 ADVs have many logistical advantages; namely, they provide a relatively simple and
1058 inexpensive way to quantify turbulence (Bluteau et al., 2011) while also being portable and
1059 robust. Furthermore, they do not require frequent calibration and are not constrained by
1060 turbidity as optical sensors are (Lohrmann et al., 1995). As well as bio-turbulence studies,
1061 ADVs are commonly used as velocity sensors in physical limnological and oceanographic
1062 studies both in the laboratory and in the field.

1063 Building upon a previous study that overlooked the quantification of turbulence
1064 (Berdalet, 1992), Berdalet et al. (2007) used a side-mounted Nortek 3D 10 MHz ADV to
1065 record current velocities at different points within a test flask placed on a shaker table.
1066 Interestingly, the ADV was mounted on the shaker table so was stationary relative to the
1067 flask. Sullivan and Swift (2003) used a Sontek ADV to quantify ε at different positions across
1068 a range of turbulent intensities. As with DPIV, the test medium was also seeded with
1069 microparticles in order to increase the acoustic backscatter and thus improve the SNR.
1070 Sullivan and Swift (2003) used two different mathematical techniques to calculate turbulence
1071 from the velocity measurements, providing a comparison of values which showed that the two

methods yielded similar results. These researchers went to lengths to ensure that the levels of turbulence generated in the experiments were analogous to those found in the ocean (namely, $\varepsilon = 10^{-8}$ $m^2 \cdot s^{-3}$ for the lower turbulence level and $\varepsilon = 10^{-4}$ $m^2 \cdot s^{-3}$ for the higher) and compared them to published ε values. A Nortek ADV was used by Guadayol et al. (2009b) to assess the differences in ε between grid- and shaker-generated turbulence. Depending on the manufacturer, the pronged head of an ADV can have a maximum diameter ~10cm in diameter thus limiting the size and shape of vessel in which it is possible to obtain measurements. In order to record the velocity in a small grid-generated turbulence vessel, this study made use of a set of bespoke 2 L and 15 L vessels that incorporated the transducer heads into the wall of the vessel itself. The vessels were constructed from Delrin plastic to limit the internal reflection from the tank walls. A larger 2500 L mesocosm tank was constructed with a grid of mesh size 10 cm so that the ADV could be deployed through the mesh without interfering with the grid mechanism. With regards to measuring velocities in the orbital shaker vessels, a custom-made, side-looking ADV was placed in the vessel, held in place by a posable arm also attached to the shaker as per Berdalet et al. (2007). Also of interest in these studies is the sampling time requirements; a longer sampling time is needed in larger vessels to resolve larger overturns. Thus, a minimum duration of 10 minutes was used in the grid tanks and 5 minutes for the shaker tables.

Laser Doppler Velocimetry

Optical Laser Doppler Velocimeters (LDV) can be used in a manner similar to acoustic Doppler velocimetry. The fluid medium is seeded with reflective beads in order to increase the SNR and then the laser is used to image particle motion within the fluid. Usefully, the technology has now advanced to the point where it is now readily commercially available with an easy installation. Unlike DPIV, only a single system is need to image 3D

flows (Eder et al., 2001). Due to the use of lasers and seeded water, this method has been incorrectly referred to as DPIV in some literature; however, similar considerations regarding the introduction of laser beams to water and the addition of seeded particles discussed should be applied.

In situations where it is difficult to place the sensor in the tank directly (due to size or presence of other apparatus), it is possible to image the fluid motion from outside the tank if the vessel is transparent and taking into account any inherent refractive effects. Peters and Gross (1994) mitigated this lensing effect by constructing a replica test tank solely for turbulence quantification. The replica tank was built out of transparent acrylic; it was surrounded by a second, square acrylic tank which was then filled with water. The outer layer of water surrounding the test tank reduced the ratio of refractive indices, thereby reducing the effects of refraction. The test tank was seeded with rutile (a mineral of titanium oxide) spheres of 2 to 3 μm diameter and particle velocities were measured in the u and v directions via a 2-axis laser anemometer.

A summary of the pros and cons associated with each method discussed in this section can be found in Table 4.

Table 4 - Summary table of different turbulence measurement techniques

Technique	Pro	Con
Particle tracking velocimetry	• High accuracy and spatial resolution • External to tank	• Redundant technology with the advent of more powerful CPUs and digital cameras
DPIV	• External to tank • Produces velocity fields over the full field of view of the camera	• Can be difficult to set up • Equipment set-up can be very costly • Potential for introduction of microplastics into water ways • Refraction effects need to be accounted for • Requires access to the tank from at least two directions • Requires two sets of equipment to visualise flows in 3D • Complex, highly technical experimental set-up
PLIF	• Can map cell concentrations as well as velocities • Can be deployed in the field in situ • External to tank • Produces velocity fields over the full field of view of the camera	• Can cause photobleaching in cells • Refraction effects need to be accounted for • Complex, highly technical experimental set-up
ADV	• Portable and robust • Can be used in turbid water • Possible to obtain multiple turbulence characteristics	• Difficult to use in tanks with moving parts • Only point measurements
LDV	• Simple installation and use • External to tank	• Refraction effects need to be accounted for • Equipment set-up can be very costly • Potential for introduction of microplastics into water ways • Only point measurements

Empirical formulae

Empirically derived formulae are used in 44% of publications to quantify turbulence (Figure 8), reflecting the high proportion of studies using Couette cylinders and shaker tables. In circumstances where the cosm is either too small or unsuitable to use measurement apparatus, it is possible to approximate the level of turbulent intensity using basic

measurements of the experimental set-up. This may be useful for researchers that do not have access to the high-cost, specialist measurement apparatus discussed previously. It is recommended to report turbulence quantification as dissipation rates (ε; m^2/s^3) to be concurrent with physical oceanographic observations in the field and thus facilitate comparison between studies. As such, Equations (3) and (5) below have been modified to output in m^2/s^3.

Shakers

Due to their small size and vessel motion, shaker experiments have typically precluded direct fluid measurement (the exception being Zirbel et al. (2000) who used PIV). As such, Peters and Marrasé (2000) were able to retrospectively estimate ε in a number of studies:

$$\varepsilon = \frac{S(d \cdot f)^3}{V} \quad (2)$$

where d = distance the vessel travels in one oscillation (m); f = frequency of oscillation (Hz), V = volume of fluid (m^3), and S = surface in contact with fluid (as derived from flask geometry; m^2). The resultant ε value will be indicative of the order of magnitude of ε, not a direct equality due to approximation in turbulent length scales.

Building upon this, Guadayol et al. (2009b) empirically formulated a relationship for ε based on direct velocity measurements across different frequencies of oscillation and orbit diameter:

$$\varepsilon = 10^{(-5.03 - 1.56\phi + f(1.71 + 1.08\phi)) - 5} \quad (3)$$

where ϕ = orbit diameter (cm). Note that Equation (3) only holds for orbital diameters between 1.4 - 3.0 cm and oscillation frequencies between 1.19 - 2.54 Hz.

Vertical grids

With regards to turbulence generated by vertically-oscillating grids, ε can be estimated as a function of grid oscillation frequency, stroke length and cosm dimensions (Peters and Marrasé, 2000).

$$\varepsilon = \left(\frac{1}{T/4}\right)\int_0^{T/4} \frac{0.7 \cdot A_{grid}}{V} u(t)^3 dt \quad (4)$$

where T = period of one oscillation (s), A_{grid} = solid area of the grid (m^2), and $u(t)$ = vertical grid velocity (m/s), as calculated from oscillation frequency and stroke length. The 0.7 coefficient is the empirically derived drag coefficient of a falling grid (Peters and Marrasé, 2000). Note that this coefficient will change accordingly with different grid geometries and configurations; given the ad hoc nature of many turbulence studies, a prudent course of action would be to calculate the drag coefficient for different grid setups.

Guadayol et al. (2009b) have also developed a series of empirical equations to describe the ε at different locations in a tank with a vertically oscillating grid. Equation (5) calculates ε at a location outside of the grid motion area:

$$\varepsilon = 2 \times 10^{-6} \cdot s^{9/2} \cdot M^{3/2} \cdot z^{-4} \cdot f^3 \quad (5)$$

where s = stroke length (cm), M = mesh size (cm), and z = distance from the centre of the oscillation (cm). Equation (5) holds for stroke lengths between 2.8 - 40 cm; mesh sizes from 0.9 - 10 cm; and, z-distances between 1 - 73 cm. See Guadayol et al. (2009b) for additional

1168 equations describing ε within the grid path as well as variations for constant and sinusoidal
1169 grid motion.
1170
1171 *Couette cylinders*
1172 In Couette cylinders, the rotational rate and shears can be easily converted to ε
1173 (Thomas and Gibson, 1990b):
1174
1175 $$\varepsilon = \nu\left(\frac{R \cdot D \cdot \pi}{60 \cdot G}\right)^2 \quad (6)$$

1176
1177 where ν = kinematic viscosity (m^2/s), R = rotational rate in revolutions per minute (rpm), D =
1178 the diameter of the outer cylinder (m), and G = the gap width (m). Note that the contents of
1179 the parentheses ($RD\pi/60G$) correspond to the value for strain (γ) in radians per second
1180 (rads/s).
1181
1182 **CONCLUSION**
1183 We have observed that experiments involving phytoplankton-turbulence interactions
1184 take many forms often dictated by budget, access to facilities and/or the background
1185 experience of the researchers themselves. This paper aimed to review the various techniques
1186 used to both generate turbulence and quantify the turbulence produced.
1187 With regards to the method of turbulence generation, most (31%) previous cosm work
1188 has been carried out using oscillating grids (as compared to aeration, Couette cylinders and
1189 shaker tables); it is our recommendation that future studies continue to make use of this
1190 method due to operational advantages and a robust set of literature and historical data for
1191 results comparison. Oscillating grids are simple, effective, and inexpensive, with 29 out of 32

studies reviewed quantifying the turbulence produced. The grids themselves can generate near-isotropic turbulence across a wide range of scales. A grid setup is relatively low-cost to implement or retrofit to existing facilities using basic variable-speed motors. Furthermore, grid setups can easily be applied to large tanks (>1m^3) to enable capturing a wider range of turbulence length scales. It is important that a mesh barrier (e.g., MacKenzie and Kiørboe (1995) be placed between the grid area and the organism to not only reduce the risk of mechanical damage but also to create a refuge region that allows the organisms respite from the turbulence. Similarly, it is important the grids are programmed accordingly to oscillate at a frequency that provides further temporal respite from maximum turbulence. Similarly, the cosm itself and the stroke-length over which the grid should oscillate should be on the order of at least one metre to properly reflect the natural length scales of vertical overturns.

With regards to our recommendation for quantification methods, Acoustic Doppler velocimeters (ADV) are both the most commonly used as well as the least complex and inexpensive of the methodologies. However, we do recognise that using an ADV within an environment with an oscillating grid does provide some logistical challenges to overcome.

Phytoplankton-turbulence interactions are complex (Figure 1); however, studies of this nature are a critical tool for helping us to better understand not only how the aquatic environment functions but also how it will respond as climate change continues to alter turbulent regimes across the planet (Hallegraeff, 2010; Hinder et al., 2012). Worringly, the number of publications of this nature has been declining in recent years (Figure 6). Only by 1) standardising future phytoplankton-turbulence experiments and 2) promoting more interdisciplinary collaboration between fluid dynamicists and aquatic ecologists will we be able to better understand the subtle, yet dominant and complex, ways that turbulence influences the microscopic lives of phytoplankton.

REFERENCES

Aguilera, J., C. Jiménez, J. M. Rodríguez-Maroto & F. X. Niell, 1994. Influence of subsidiary energy on growth of *Dunaliella viridis* Teodoresco: the role of extra energy in algal growth. Journal of Applied Phycology 6(3):323-330.

Alcaraz, M., E. Saiz, C. Marrasé & D. Vaqué, 1988. Effects of turbulence on the development of phytoplankton biomass and copepod populations in marine microcosms. Marine Ecology Progress Series 49:117 - 125.

Alexander, A. C., E. Luiker, M. Finley & J. M. Culp, 2016. Chapter 8 - Mesocosm and Field Toxicity Testing in the Marine Context. In Blasco, J., P. M. Chapman, O. Campana & M. Hampel (eds) Marine Ecotoxicology. Academic Press, 239-256.

Alldredge, A. L., T. C. Granata, C. C. Gotschalk & T. D. Dickey, 1990. The physical strength of marine snow and its implications for particle disaggregation in the ocean. Limnology and Oceanography 35(7):1415-1428.

Arin, L., C. Marrasé, M. Maar, F. Peters, M. M. Sala & M. Alcaraz, 2002. Combined effects of nutrients and small-scale turbulence in a microcosm experiment. I. Dynamics and size distribution of osmotrophic plankton. Aquatic Microbial Ecology 29(1):51-61.

Bakus, G., J., 1973. Some effects of turbulence and light on competition between two species of phytoplankton. Investigación Pesquera 37:87-100.

Båmstedt, U. & H. Larsson, 2018. An indoor pelagic mesocosm facility to simulate multiple water-column characteristics. International Aquatic Research 10(1):13-29.

Banse, K., 1991. Rates of phytoplankton cell division in the field and in iron enrichment experiments. Limnology and Oceanography 36(8):1886-1898.

Beauvais, S., M. L. Pedrotti, J. Egge, K. Iversen & C. Marrasé, 2006. Effects of turbulence on TEP dynamics under contrasting nutrient conditions: Implications for aggregation and sedimentation processes. Marine Ecology Progress Series 323:47-57.

Behm, J. E., B. R. Waite, S. T. Hsieh & M. R. Helmus, 2018. Benefits and limitations of three-dimensional printing technology for ecological research. BioMed Central Ecology 18(1):32-32.

Berdalet, E., 1992. Effects of turbulence on the marine dinoflagellate *Gymnodinium nelsonii*. Journal of Phycology 28(3):267-272.

Berdalet, E. & M. Estrada, 1993. Effects of turbulence on several phytoplankton species. In Smayda, T. J. & Y. Shimizu (eds) Toxic Phytoplankton Blooms in the Sea. Developments in Marine Biology, vol 3. Elsevier, Amsterdam, The Netherlands, 737 - 740.

Berdalet, E., F. Peters, V. L. Koumandou, C. Roldán, Ò. Guadayol & M. Estrada, 2007. Species-specific physiological response of dinoflagellates to quantified small-scale turbulence. Journal of Phycology 43(5):965-977.

Bergkvist, J., I. Klawonn, M. J. Whitehouse, G. Lavik, V. Brüchert & H. Ploug, 2018. Turbulence simultaneously stimulates small- and large-scale CO2 sequestration by chain-forming diatoms in the sea. Nature Communications 9(1).

Bienfang, P. K., P. J. Harrison & L. M. Quarmby, 1982. Sinking rate response to depletion of nitrate, phosphate and silicate in four marine diatoms. Marine Biology 67(3):295-302.

Bluteau, C. E., N. L. Jones & G. N. Ivey, 2011. Estimating turbulent kinetic energy dissipation using the inertial subrange method in environmental flows. Limnology and Oceanography: Methods 9(7):302-321.

Chen, D., K. Muda, K. Jones, J. Leftly & P. Stansby, 1998. Effect of shear on growth and motility of *Alexandrium minutum* Halim, a red-tide dinoflagellate. In Reguera, B., J. Blanco, M. L. Fernández & T. Wyatt (eds) Harmful algae. Xunta de Galicia and Intergovernmental Oceanographic Commision of UNESCO, Vigo, Galicia, Spain, 352-355.

Coble, P. G., 2007. Marine Optical Biogeochemistry: The Chemistry of Ocean Color. Chemical Reviews 107(2):402-418.

Couette, M., 1890. Distinction de deux régimes dans le mouvement des fluides. Journal de Physique Théorique et Appliquée 9(1):414-424.

Cózar, A. & F. Echevarría, 2005. Size structure of the planktonic community in microcosms with different levels of turbulence. Scientia Marina 69(2):187-197.

Crimaldi, J. P., 2008. Planar laser induced fluorescence in aqueous flows. Experiments in Fluids 44(6):851-863.

Crossland, N. O. & T. W. La Point, 1992. The design of mesocosm experiments. Environmental Toxicology and Chemistry 11(1):1-4.

Davis, E. A., J. Dedrick, C. S. French, H. W. Milner, J. Myers, J. H. C. Smith & H. A. Spoehr, 1953. Laboratory experiments on Chlorella culture at the Carnegie Institution of Washington department of plant biology. In Burlew, J. S. (ed) Algal Culture from Laboratory to Pilot Plant. 5th edn. Carnegie Institution of Washington, Washington DC, 105-153.

Dawidowicz, P., 1990. The effect of *Daphnia* on filament length of blue-green algae. Hydrobiologia 191(1):265-268.

Delaney, M. P., 2003. Effects of temperature and turbulence on the predator-prey interactions between a heterotrophic flagellate and a marine bacterium. Microbial ecology 45(3):218-225.

Dempsey, H. P., 1982. The effects of turbulence on three algae: *Skeletonema costatum, Gonyaulax tamarensis, Heterocapsa triquentra*. Massachusetts Institute of Technology.

Dolan, J. R., N. Sall, A. Metcalfe & B. Gasser, 2003. Effects of turbulence on the feeding and growth of a marine oligotrich ciliate. Aquatic Microbial Ecology 31(2):183-192.

Donaghay, P. L. & E. Klos, 1985. Physical, chemical and biological responses to simulated wind and tidal mixing in experimental marine ecosystems. Marine Ecology Progress Series 26(1/2):35-45.

Eder, A., B. Durst & M. Jordan, 2001. Laser-Doppler Velocimetry — Principle and Application to Turbulence Measurements. In Mayinger, F. & O. Feldmann (eds) Optical Measurements: Techniques and Applications. Springer, Berlin, Heidelberg, 117-138.

Eppley, R. W., P. Koeller & G. T. Wallace, 1978. Stirring influences the phytoplankton species composition within enclosed columns of coastal sea water. Journal of Experimental Marine Biology and Ecology 32(3):219-239.

Escaravage, V., L. P. M. J. Wetsteyn, T. C. Prins, A. J. Pouwer, A. de Kruyff, M. Vink-Lievaart, C. M. van der Voom, J. C. H. Peeters & A. C. Smaal, 1997. The impact of marine eutrophication on phytoplankton, zooplankton and benthic suspension feeders. Stratification in mesocosms, a pilot experiment. Ministerie van Verkeer en Waterstaat, The Netherlands, 52.

Estrada, M., M. Alcaraz & C. Marrasé, 1987. Effects of turbulence on the composition of phytoplankton assemblages in marine microcosms. Marine Ecology Progress Series 38:267-281.

Fogg, G. E. & Than-Tun, 1960. Interrelations of photosynthesis and assimilation of elementary nitrogen in a blue-green alga. Proceedings of the Royal Society of London Series B Biological Sciences 153(950):111-127.

Fraisse, S., M. Bormans & Y. Lagadeuc, 2015. Turbulence effects on phytoplankton morphofunctional traits selection. Limnology and Oceanography 60(3):872-884.

Franks, P. J. S., 2001. Turbulence avoidance: An alternate explanation of turbulence-enhanced ingestion rates in the field. Limnology and Oceanography 46(4):959-963.

Franks, P. J. S. & J. S. Jaffe, 2008. Microscale variability in the distributions of large fluorescent particles observed in situ with a planar laser imaging fluorometer. Journal of Marine Systems 69(3):254-270.

Fuchs, H. L. & G. P. Gerbi, 2016. Seascape-level variation in turbulence- and wave-generated hydrodynamic signals experienced by plankton. Progress in Oceanography 141:109-129.

Garrison, H. S. & K. W. Tang, 2014. Effects of episodic turbulence on diatom mortality and physiology, with a protocol for the use of Evans Blue stain for live–dead determinations. Hydrobiologia 738(1):155-170.

Gibson, C. H. & W. H. Thomas, 1995. Effects of turbulence intermittency on growth inhibition of a red tide dinoflagellate, *Gonyaulax polyedra* Stein. Journal of Geophysical Research: Oceans 100(C12):24841-24846.

Gonzalez-Fernandez, C., J. Toullec, C. Lambert, N. Le Goic, M. Seoane, B. Moriceau, A. Huvet, M. Berchel, D. Vincent, L. Courcot, P. Soudant & I. Paul-Pont, 2019. Do transparent exopolymeric particles (TEP) affect the toxicity of nanoplastics on *Chaetoceros neogracile*? Environmental Pollution 250:873-882.

Grobbelaar, J. U., 1989. Do light/dark cycles of medium frequency enhance phytoplankton productivity? Journal of Applied Phycology 1(4):333-340.

Guadayol, O., C. Marrasé, F. Peters, E. Berdalet, N. Roldá & A. Sabata, 2009a. Responses of coastal osmotrophic planktonic communities to simulated events of turbulence and nutrient load throughout a year. Journal of Plankton Research 31(6):583-600.

Guadayol, Ò., F. Peters, J. E. Stiansen, C. Marrasé & A. Lohrmann, 2009b. Evaluation of oscillating grids and orbital shakers as means to generate isotropic and homogeneous small-scale turbulence in laboratory enclosures commonly used in plankton studies. Limnology and Oceanography: Methods 7(APR.):287-303.

Guasto, J. S., R. Rusconi & R. Stocker, 2012. Fluid mechanics of planktonic microorganisms. Annual Review of Fluid Mechanics 44:373 - 400.

Hallegraeff, G. M., 2010. Ocean climate change, phytoplankton community responses, and harmful algal blooms: a formidable predictive challenge. Journal of Phycology 46(2):220-235.

Havskum, H., 2003. Effects of small-scale turbulence on interactions between the heterotrophic dinoflagellate *Oxyrrhis marina* and its prey, *Isochrysis* sp. Ophelia 57(3):125-135.

Havskum, H. & P. J. Hansen, 2006. Net growth of the bloom-forming dinoflagellate *Heterocapsa triquetra* and pH: Why turbulence matters. Aquatic Microbial Ecology 42(1):55-62.

Havskum, H., P. J. Hansen & E. Berdalet, 2005. Effect of turbulence on sedimentation and net population growth of the dinoflagellate *Ceratium tripos* and interactions with its predator, *Fragilidium subglobosum*. Limnology and Oceanography 50(5):1543-1551.

Hellung-Larsen, P. & I. Lyhne, 1992. Effect of shaking on the growth of diluted cultures of *Tetrahymena*. The Journal of Protozoology 39(2):345-349.

Hinder, S. L., G. C. Hays, M. Edwards, E. C. Roberts, A. W. Walne & M. B. Gravenor, 2012. Changes in marine dinoflagellate and diatom abundance under climate change. Nature Climate Change 2(4):271-275.

Hondzo, M. M., A. Kapur & C. A. Lembi, 1997. The effect of small-scale fluid motion on the green alga *Scenedesmus quadricauda*. Hydrobiologia 364(2):225-235.

Howarth, R. W., T. Butler, K. Lunde, D. Swaney & C. R. Chu, 1993. Turbulence and planktonic nitrogen fixation: a mesocosm experiment. Limnology and Oceanography 38(8):1696-1711.

Hoyer, K., M. Holzner, B. Lüthi, M. Guala, A. Liberzon & W. Kinzelbach, 2005. 3D scanning particle tracking velocimetry. Experiments in Fluids 39(5):923.

Huisman, J., P. Van Oostveen & F. J. Weissing, 1999. Critical depth and critical turbulence: Two different mechanisms for the development of phytoplankton blooms. Limnology and Oceanography 44(7):1781-1787.

Iversen, K. R., R. Primicerio, A. Larsen, J. K. Egge, F. Peters, Ó. Guadayol, A. Jacobsen, H. Havskum & C. Marrasé, 2009. Effects of small-scale turbulence on lower trophic levels under different nutrient conditions. Journal of Plankton Research 32(2):197-208.

Juhl, A. R. & M. I. Latz, 2002. Mechanisms of fluid shear-induced inhibition of population growth in a red-tide dinoflagellate. Journal of Phycology 38(4):683-694.

Juhl, A. R., V. L. Trainer & M. I. Latz, 2001. Effect of fluid shear and irradiance on population growth and cellular toxin content of the dinoflagellate *Alexandrium fundyense*. Limnology and Oceanography 46(4):758-764.

Juhl, A. R., V. Velazquez & M. I. Latz, 2000. Effect of growth conditions on flow-induced inhibition of population growth of a red-tide dinoflagellate. Limnology and Oceanography 45(4):905-915.

Kaku, V. J., M. C. Boufadel & A. D. Venosa, 2006. Evaluation of mixing energy in laboratory flasks used for dispersant effectiveness testing. Journal of Environmental Engineering 132(1):93-101.

Kangas, P. C. & W. H. Adey, 2008. Mesocosm Management. In Jørgensen, S. E. & B. D. Fath (eds) Encyclopedia of Ecology. Academic Press, Oxford, 2308-2313.

Karp-Boss, L., E. Boss & P. A. Jumars, 2000. Motion of dinoflagellates in a simple shear flow. Limnology and Oceanography 45(7):1594-1602.

Karp-Boss, L. & P. A. Jumars, 1998. Motion of diatom chains in steady shear flow. Limnology and Oceanography 43(8):1767-1773.

Katija, K., 2012. Biogenic inputs to ocean mixing. The Journal of Experimental Biology 215(6):1040-1049.

Kilham, P., 1971. A hypothesis concerning silica and the freshwater planktonic diatoms. Limnology and Oceanography 16(1):10-18.

Kiørboe, T., 1993. Turbulence, phytoplankton cell size, and the structure of pelagic food webs. Advances in Marine Biology 29:1-72.

Kiørboe, T., K. P. Andersen & H. G. Dam, 1990. Coagulation efficiency and aggregate formation in marine phytoplankton. Marine Biology 107(2):235-245.

Kirke, B. K., Pumping downwards to prevent algal blooms. In: IWA 2nd World Water Congress, Berlin, 2001.

Köhler, J., 1997. Measurement of in situ growth rates of phytoplankton under conditions of simulated turbulence. Journal of Plankton Research 19(7):849-862.

Kromkamp, J., F. Schanz, M. Rijkeboer, E. Berdalet, B. Kim & H. J. Gons, 1992. Influence of the mixing regime on algal photosynthetic performance in laboratory scale enclosures. Hydrobiologia 238(1):111-118.

Latz, M. I., J. Allen, S. Sarkar & J. Rohr, 2009. Effect of fully characterized unsteady flow on population growth of the dinoflagellate *Lingulodinium polyedrum*. Limnology and Oceanography 54(4):1243-1256.

Latz, M. I., J. F. Case & R. L. Gran, 1994. Excitation of bioluminescence by laminar fluid shear associated with simple Couette flow. Limnology and Oceanography 39(6):1424-1439.

Latz, M. I., J. C. Nauen & J. Rohr, 2004. Bioluminescence response of four species of dinoflagellates to fully developed pipe flow. Journal of Plankton Research 26(12):1529-1546.

Latz, M. I. & J. Rohr, 1999. Luminescent response of the red tide dinoflagellate *Lingulodinium polyedrum* to laminar and turbulent flow. Limnology and Oceanography 44(6):1423-1435.

Laws, E. A., K. L. Terry, J. Wickman & M. S. Chalup, 1983. A simple algal production system designed to utilize the flashing light effect. Biotechnology and Bioengineering 25(10):2319-2335.

Lazier, J. R. N. & K. H. Mann, 1989. Turbulence and the diffusive layers around small organisms. Deep Sea Research Part A Oceanographic Research Papers 36(11):1721-1733.

Leeuw, T., E. S. Boss & D. L. Wright, 2013. In situ measurements of phytoplankton fluorescence using low cost electronics. Sensors 13(6):7872-7883.

Leterme, S. C., I. Kesaulya, J. G. Mitchell & L. Seuront, 2008. The impact of turbulence and phytoplankton dynamics on foam formation, seawater viscosity and chlorophyll concentrations in the eastern English Channel. Oceanologia 50(2):167-182.

Linares, M. C., 2015. Effects of turbulence and laser exposure on phytoplankton behavior. Universitat Politecnica de Catalunya.

Liu, F., L. Zeng, Y. H. Wu, B. Baoligao & X. Chen, 2017. Vertical distribution of motile phytoplankton in density currents. In: Li, P. (ed) 3rd International Conference on Water Resource and Environment (WRE 2017), Qingdao, China, 26–29 June 2017. IOP Conference Series: Earth and Environmental Science, vol 82. IOP Publishing, p 012073.

Llaveria, G., E. Garcés, O. N. Ross, R. I. Figueroa, N. Sampedro & E. Berdalet, 2010. Small-scale turbulence can reduce parasite infectivity to dinoflagellates. Marine Ecology Progress Series 412:45-56.

Lohrmann, A., R. Cabrera, G. Gelfenbaum & J. Haines, 1995. Direct measurements of Reynolds stress with an acoustic Doppler velocimeter. In: Anderson, S.P., G.F. Appell & A. J. Williams III (eds) Proceedings of the IEEE Fifth Working Conference on Current Measurement, St. Petersburg, FL, USA, 7-9 Feb 1995. IEEE, p 205-210.

Long, J. D., G. W. Smalley, T. Barsby, J. T. Anderson & M. E. Hay, 2007. Chemical cues induce consumer-specific defenses in a bloom-forming marine phytoplankton. Proceedings of the National Academy of Sciences 104(25):10512-10517.

Lürling, M., 1998. Effect of grazing-associated infochemicals on growth and morphological development in *Scenedesmus acutus* (Chlorophyceae). Journal of Phycology 34(4):578-586.

Maar, M., L. Arin, R. Simó, M.-M. Sala, F. Peters & C. Marrasé, 2002. Combined effects of nutrients and small-scale turbulence in a microcosm experiment. II. Dynamics of organic matter and phosphorus. Aquatic Microbial Ecology 29(1):63-72.

MacKenzie, B. R. & T. Kiørboe, 1995. Encounter rates and swimming behavior of pause-travel and cruise larval fish predators in calm and turbulent laboratory environments. Limnology and Oceanography 40(7):1278-1289.

Margalef, R., 1997. Turbulence and marine life. In: Marrasé, C., E. Saiz & J. M. Redondo (eds) Scientia Marina: Lectures on plankton and turbulence. Vol 61 (SUPPL.1), 109-123.

Marrasé, C., J. H. Costello, T. Granata & J. R. Strickler, 1990. Grazing in a turbulent environment: Energy dissipation, encounter rates, and efficacy of feeding currents in *Centropages hamatus*. Proceedings of the National Academy of Sciences of the United States of America 87(5):1653-1657.

Martin, J. H. & R. Michael Gordon, 1988. Northeast Pacific iron distributions in relation to phytoplankton productivity. Deep Sea Research Part A Oceanographic Research Papers 35(2):177-196.

Martínez, R. A., A. Calbet & E. Saiz, 2017. Effects of small-scale turbulence on growth and grazing of marine microzooplankton. Aquatic Sciences 80(1).

Matheson, F. E., 2008. Microcosms. In Jørgensen, S. E. & B. D. Fath (eds) Encyclopedia of Ecology. Academic Press, Oxford, 2393-2397.

Metcalfe, A. M., T. J. Pedley & T. F. Thingstad, 2004. Incorporating turbulence into a plankton foodweb model. Journal of Marine Systems 49(1-4):105-122.

Moisander, P. H., J. L. Hench, K. Kononen & H. W. Paerl, 2002. Small-scale shear effects on heterocystous cyanobacteria. Limnology and Oceanography 47(1):108-119.

Musielak, M. M., L. E. E. Karp-Boss, P. A. Jumars & L. J. Fauci, 2009. Nutrient transport and acquisition by diatom chains in a moving fluid. Journal of Fluid Mechanics 638:401-421.

Naselli-Flores, L., T. Zohary & J. Padisák, 2020. Life in suspension and its impact on phytoplankton morphology: an homage to Colin S. Reynolds. Hydrobiologia 848:7-30 (2021).

Nedbal, L., V. Tichý, F. Xiong & J. U. Grobbelaar, 1996. Microscopic green algae and cyanobacteria in high-frequency intermittent light. Journal of Applied Phycology 8(4):325-333.

Nejstgaard, J., C. , L.-J. Naustvoll & A. Sazhin, 2001a. Correcting for underestimation of microzooplankton grazing in bottle incubation experiments with mesozooplankton. Marine Ecology Progress Series 221:59-75.

Nejstgaard, J., C., B. H. Hygum, L.-J. Naustvoll & U. Båmstedt, 2001b. Zooplankton growth, diet and reproductive success compared in simultaneous diatom- and flagellate-microzooplankton-dominated plankton blooms. Marine Ecology Progress Series 221:77-91.

Nerheim, S., J. E. Stiansen & H. Svendsen, 2002. Grid-generated turbulence in a mesocosm experiment. Hydrobiologia 484:61-73.

Odum, E. P., 1984. The Mesocosm. BioScience 34(9):558-562.

Okubo, A., 1976. Remarks on the use of 'diffusion diagrams' in modeling scale-dependent diffusion. Deep Sea Research and Oceanographic Abstracts 23(12):1213-1214.

Oviatt, C. A., 1981. Effects of different mixing schedules on phytoplankton, zooplankton and nutrients in marine microcosms. Marine Ecology Progress Series 4:57-67.

Paczkowska, J., O. F. Rowe, L. Schlüter, C. Legrand, B. Karlson & A. Andersson, 2017. Allochthonous matter: An important factor shaping the phytoplankton community in the Baltic Sea. Journal of Plankton Research 39(1):23-34.

Padisák, J., É. Soróczki-Pintér & Z. Rezner, 2003. Sinking properties of some phytoplankton shapes and the relation of form resistance to morphological diversity of plankton - an experimental study. Hydrobiolgia 500:243-257.

Pahlow, M., U. Riebesell & D. A. Wolf-Gladrow, 1997. Impact of cell shape and chain formation on nutrient acquisition by marine diatoms. Limnology and Oceanography 42(8):1660-1672.

Pannard, A., M. Bormans, S. Lefebvre, P. Claquin & Y. Lagadeuc, 2007. Phytoplankton size distribution and community structure: influence of nutrient input and sedimentary loss. Journal of Plankton Research 29(7):583-598.

Parsons, T. R., P. J. Harrison & R. Waters, 1978. An experimental simulation of changes in diatom and flagellate blooms. Journal of Experimental Marine Biology and Ecology 32(3):285-294.

Pasciak, W. J. & J. Gavis, 1975. Transport limited nutrient uptake rates in *Ditylum brightwellii*. Limnology and Oceanography 20(4):604-617.

Peters, F., L. Arin, C. Marrasé, E. Berdalet & M. M. Sala, 2006. Effects of small-scale turbulence on the growth of two diatoms of different size in a phosphorus-limited medium. In: Peters, F. & C. Hannah (eds) Workshop on Future Directions in Modelling Physical-Biological Interactions (WKFDPBI), Barcelona, Catalunya, Spain, 7-9 March 2004. Journal of Marine Systems 61(3-4):134-148.

Peters, F., J. W. Choi & T. Gross, 1996. *Paraphysomonas imperforata* (Protista, Chrysomonadida) under different turbulence levels: feeding, physiology and energetics. Marine Ecology Progress Series 134:235-245.

Peters, F. & T. Gross, 1994. Increased grazing rates of microplankton in response to small-scale turbulence. Marine Ecology Progress Series 115(3):299-308.

Peters, F. & C. Marrasé, 2000. Effects of turbulence on plankton: An overview of experimental evidence and some theoretical considerations. Marine Ecology Progress Series 205:291-306.

Peters, F., C. Marrasé, H. Havskum, F. Rassoulzadegan, J. Dolan, M. Alcaraz & J. M. Gasol, 2002. Turbulence and the microbial food web: Effects on bacterial losses to predation and on community structure. Journal of Plankton Research 24(4):321-331.

Peters, F. & J. M. Redondo, 1997. Turbulence generation and measurement: Application to studies on plankton. In: Marrasé, C., E. Saiz & J. M. Redondo (eds) Scientia Marina: Lectures on plankton and turbulence. Vol 61 (SUPPL.1), 205-228.

Petersen, J. E., L. P. Sanford & W. M. Kemp, 1998. Coastal plankton responses to turbulent mixing in experimental ecosystems. Marine Ecology Progress Series 171:23-41.

Pollingher, U. & E. Zemel, 1981. In situ and experimental evidence of the influence of turbulence on cell division processes of *Peridinium cinctum* forma *westii* (Lemm.) Lefèvre. British Phycological Journal 16(3):281-287.

Prairie, J. C., K. R. Sutherland, K. J. Nickols & A. M. Kaltenberg, 2012. Biophysical interactions in the plankton: A cross-scale review. Limnology and Oceanography: Fluids and Environments 2(1):121-145.

Pringle, J. M., 2007. Turbulence avoidance and the wind-driven transport of plankton in the surface Ekman layer. Continental Shelf Research 27(5):670-678.

Raffel, M., C. E. Willert, F. Scarano, C. J. Kähler, S. T. Wereley & J. Kompenhans, 2018. Particle image velocimetry: a practical guide. Springer.

Regel, R. H., J. D. Brookes, G. G. Ganf & R. W. Griffiths, 2004. The influence of experimentally generated turbulence on the Mash01 unicellular *Microcystis aeruginosa* strain. Hydrobiologia 517(1):107-120.

Reynolds, C. S., 2009. Biological–Physical Interactions. In Likens, G. E. (ed) Encyclopedia of Inland Waters. Academic Press, Oxford, 515-521.

Richmond, A. & A. Vonshak, 1978. Spirulina culture in Israel. Archiv für Hydrobiologie - Beihefte Ergebnisse der Limnologie 11:274 - 280.

Rijkeboer, M., F. de Bles & H. J. Gons, 1990. Laboratory scale enclosure: concept, construction and operation. Journal of Plankton Research 12(1):231-244.

Rohr, J., J. Allen, J. Losee & M. I. Latz, 1997. The use of bioluminescence as a flow diagnostic. Physics Letters A 228(6):408-416.

Rohr, J., M. Hyman, S. Fallon & M. I. Latz, 2002. Bioluminescence flow visualization in the ocean: an initial strategy based on laboratory experiments. Deep Sea Research Part I: Oceanographic Research Papers 49(11):2009-2033.

Rohr, J., J. Losee & J. Hoyt, 1990. Stimulation of bioluminescence by turbulent pipe flow. Deep Sea Research Part A, Oceanographic Research Papers 37(10):1639-1646.

Ross, O. N. & J. Sharples, 2007. Phytoplankton motility and the competition for nutrients in the thermocline. Marine Ecology Progress Series 347:21-38.

Ross, O. N. & J. Sharples, 2008. Swimming for survival : A role of phytoplankton motility in a stratified turbulent environment. Journal of Marine Systems 70(3-4):248-262.

Rothschild, B. J. & T. R. Osborn, 1988. Small-scale turbulence and plankton contact rates. Journal of Plankton Research 10(3):465-474.

Saiz, E. & M. Alcaraz, 1992. Free-swimming behaviour of *Acartia clausi* (Copepoda: Calanoida) under turbulent water movement. Marine Ecology Progress Series 80(2-3):229-236.

Saiz, E. & T. Kiørboe, 1995. Predatory and suspension feeding of the copepod Acartia tonsa in turbulent environments. Oceanographic Literature Review 43(1):59.

Sanford, L. P., 1997. Turbulent mixing in experimental ecosystem studies. Marine Ecology Progress Series 161:265-293.

Santschi, P. H., 1985. The MERL mesocosm approach for studying sediment-water interactions and ecotoxicology. Environmental Technology Letters 6(1-11):335-350.

Sato, T., D. Yamada & S. Hirabayashi, 2010. Development of virtual photobioreactor for microalgae culture considering turbulent flow and flashing light effect. Energy Conversion and Management 51(6):1196-1201.

Savidge, G., 1981. Studies of the effects of small-scale turbulence on phytoplankton. Journal of the Marine Biological Association of the United Kingdom 61(2):477-488.

Scarano, F., 2012. Tomographic PIV: principles and practice. Measurement Science and Technology 24(1):012001.

Schapira, M., L. Seuront & V. Gentilhomme, 2006. Effects of small-scale turbulence on *Phaeocystis globosa* (Prymnesiophyceae) growth and life cycle. Journal of Experimental Marine Biology and Ecology 335(1):27-38.

Schöne, H., 1970. Untersuchungen zur ökologischen Bedeutung des Seegangs für das Plankton mit besonderer Berücksichtigung mariner Kieselalgen. Internationale Revue der gesamten Hydrobiologie und Hydrographie 55(4):595-677.

Schwartz, E. R., R. X. Poulin, N. Mojib & J. Kubanek, 2016. Chemical ecology of marine plankton. Natural Product Reports 33(7):843-860.

Sengupta, A., F. Carrara & R. Stocker, 2017. Phytoplankton can actively diversify their migration strategy in response to turbulent cues. Nature 543:555-558.

Simoncelli, S., S. J. Thackeray & D. J. Wain, 2019. Effect of temperature on zooplankton vertical migration velocity. Hydrobiologia 829(1):143-166.

Smayda, T. J. & C. S. Reynolds, 2001. Community assembly in marine phytoplankton: Application of recent models to harmful dinoflagellate blooms. Journal of Plankton Research 23(5):447-461.

Smith, B. C. & A. Persson, 2005. Synchronization of encystment of *Scrippsiella lachrymosa* (Dinophyta). Journal of Applied Phycology 17(4):317-321.

Solomon, K. R. & M. Hanson, 2014. Mesocosms and Microcosms (Aquatic) Encyclopedia of Toxicology: Third Edition. 223-226.

Sonntag, N. C. & T. R. Parsons, 1979. Mixing an enclosed, 1300m^3 water column: effects on the planktonic food web. Journal of Plankton Research 1(1):85-102.

Staehr, P. A. & K. Sand-Jensen, 2006. Seasonal changes in temperature and nutrient control of photosynthesis, respiration and growth of natural phytoplankton communities. Freshwater Biology 51(2):249-262.

Steele, J. H., D. M. Farmer & E. W. Henderson, 1977. Circulation and temperature structure in large marine enclosures. Journal of the Fisheries Research Board of Canada 34(8):1095-1104.

Stoecker, D. K., A. Long, S. E. Suttles & L. P. Sanford, 2006. Effect of small-scale shear on grazing and growth of the dinoflagellate *Pfiesteria piscicida*. Harmful Algae 5(4):407-418.

Stokes, M. D., G. B. Deane, M. I. Latz & J. Rohr, 2004. Bioluminescence imaging of wave-induced turbulence. Journal of Geophysical Research: Oceans 109(C1):1-8.

Striebel, M., L. Kirchmaier & P. Hingsamer, 2013. Different mixing techniques in experimental mesocosms—does mixing affect plankton biomass and community composition? Limnology and Oceanography: Methods 11(4):176-186.

Sullivan, J. M. & E. Swift, 2003. The effect of small-scale turbulence on net growth rate and size of ten species of marine dinoflagellates. Journal of Phycology 39:83-94.

Sullivan, J. M., E. Swift, P. L. Donaghay & J. E. B. Rines, 2003. Small-scale turbulence affects the division rate and morphology of two red-tide dinoflagellates. Harmful Algae 2(3):183-199.

Svensen, C., J. K. Egge & J. E. Stiansen, 2001. Can silicate and turbulence regulate the vertical flux of biogenic matter? A mesocosm study. Marine Ecology Progress Series 217:67-80.

Sverdrup, H. U., 1953. On conditions for the vernal blooming of phytoplankton. ICES Journal of Marine Science 18(3):287-295.

Talling, J. F., 1960. Comparative laboratory and field studies of photosynthesis by a marine planktonic diatom. Limnology and Oceanography 5(1):62-77.

Thomas, W. H. & C. H. Gibson, 1990a. Effects of small-scale turbulence on microalgae. Journal of Applied Phycology 2(1):71-77.

Thomas, W. H. & C. H. Gibson, 1990b. Quantified small-scale turbulence inhibits a red tide dinoflagellate, *Gonyaulax polyedra* Stein. Deep Sea Research Part A Oceanographic Research Papers 37(10):1583-1593.

Thomas, W. H. & C. H. Gibson, 1992. Effects of quantified small-scale turbulence on the dinoflagellate, *Gymnodium sanguineum* (*splendens*): contrasts with *Gonyaulax* (*Lingulodinium*) *polyedra*, and the fishery implication. Deep Sea Research Part A Oceanographic Research Papers 39(7):1429-1437.

Thomas, W. H., D. L. R. Seibert, M. Alden, A. Neori & P. Eldridge, 1984a. Yields, photosynthetic efficiencies and proximate composition of dense marine microalgal cultures. I. Introduction and *Phaeodactylum tricornutum* experiments. Biomass 5(3):181-209.

Thomas, W. H., D. L. R. Seibert, M. Alden, A. Neori & P. Eldridge, 1984b. Yields, photosynthetic efficiencies and proximate composition of dense marine microalgal cultures. II. *Dunaliella primolecta* and *Tetraselmis suecica* experiments. Biomass 5(3):211-225.

Thomas, W. H., D. L. R. Seibert, M. Alden, A. Neori & P. Eldridge, 1984c. Yields, photosynthetic efficiencies and proximate composition of dense marine microalgal cultures. III. *Isochrysis* sp. and *Monallantus salina* experiments and comparative conclusions. Biomass 5(4):299-316.

Thomas, W. H., C. T. Tynan & C. H. Gibson, 1997. Turbulence-phytoplankton interrelationships. In Round, F. E. & D. J. Chapman (eds) Progress in Phycological Research. vol 12. Biopress Ltd, Bristol, UK, 283-324.

Tropea, C. & A. L. Yarin, 2007. Springer handbook of experimental fluid mechanics. Springer Science & Business Media.

Turkoglu, M., 2013. Red tides of the dinoflagellate *Noctiluca scintillans* associated with eutrophication in the Sea of Marmara (the Dardanelles, Turkey). Oceanologia 55(3):709-732.

Tuttle, R. C. & A. R. Loeblich, 1975. An optimal growth medium for the dinoflagellate *Crypthecodinium cohnii*. Phycologia 14(1):1-8.

Tynan, C. T., 1993. The effects of small-scale turbulence on dinoflagellates. University of California, San Diego.

Visser, P. M., B. W. Ibelings, M. Bormans & J. Huisman, 2016. Artificial mixing to control cyanobacterial blooms: a review. Aquatic Ecology 50(3):423-441.

Waller, W. T. & H. J. Allen, 2008. Acute and Chronic Toxicity. In Jørgensen, S. E. & B. D. Fath (eds) Encyclopedia of Ecology. Academic Press, Oxford, 32-43.

Walsby, A. E., 1971. Pressure relationships of gas vacuoles. Proceedings of the Royal Society of London B 178:301-326.

Warnaars, T. A., M. Hondzo & M. A. Carper, 2006. A desktop apparatus for studying interactions between microorganisms and small-scale fluid motion. Hydrobiologia 563(1):431-443.

Waterhouse, A. F., J. A. MacKinnon, J. D. Nash, M. H. Alford, E. Kunze, H. L. Simmons, K. L. Polzin, L. C. S. Laurent, O. M. Sun, R. Pinkel, L. D. Talley, C. B. Whalen, T. N. Huussen, G. S. Carter, I. Fer, S. Waterman, A. C. N. Garabato, T. B. Sanford & C. M. Lee, 2014. Global patterns of diapycnal mixing from measurements of the turbulent dissipation rate. Journal of Physical Oceanography 44(7):1854-1872.

Webster, D. R., A. Brathwaite & J. Yen, 2004. A novel laboratory apparatus for simulating isotropic oceanic turbulence at low Reynolds number. Limnology and Oceanography: Methods 2(JAN.):1-12.

Webster, D. R., P. J. W. Roberts & L. Ra'ad, 2001. Simultaneous DPTV/PLIF measurements of a turbulent jet. Experiments in Fluids 30(1):65-72.

White, A. W., 1976. Growth inhibition caused by turbulence in the toxic marine dinoflagellate *Gonyaulax excavata*. Journal of the Fisheries Research Board of Canada 33(11):2598-2602.

Wüest, A. & A. Lorke, 2003. Small-scale hydrodynamics in lakes. Annual Review of fluid mechanics 35(1):373-412.

Xu, D. & J. Chen, 2013. Accurate estimate of turbulent dissipation rate using PIV data. Experimental Thermal and Fluid Science 44:662-672.

Yeung, P. K. K. & J. T. Y. Wong, 2003. Inhibition of cell proliferation by mechanical agitation involves transient cell cycle arrest at G1 phase in dinoflagellates. Protoplasma 220(3):173-178.

Yousif, E. & R. Haddad, 2013. Photodegradation and photostabilization of polymers, especially polystyrene: review. Springerplus 2:398-398.

Zhou, J., X. Han, B. Qin, C. Casenave & G. Yang, 2016. Response of zooplankton community to turbulence in large, shallow Lake Taihu: a mesocosm experiment. Fundamental and Applied Limnology / Archiv für Hydrobiologie 187(4):325-324.

Zirbel, M. J., F. Veron & M. I. Latz, 2000. The reversible effect of flow on the morphology of *Ceratocorys horrida* (Peridiniales, Dinophyta). Journal of Phycology 36(1):46-58.

APPENDIX 1 - Lesser-used turbulence-generation techniques

Having covered the main techniques used to generate turbulence in the laboratory, it is also worth discussing more novel or lesser-used techniques, including pumping, magnetic stirrers, rotating chambers, wave tanks, impellers/propellers, paddles, dialysis cylinders, and convective mixing.

Pumping: As is common practice in aquaria, water may be introduced via a pump. This manner of turbulence generation is unrepresentative of natural turbulence as mixing would be greatest adjacent to the outflow and would quickly attenuate with distance (Sanford, 1997). Depending on the length of study, the effectiveness of the pumps may become reduced with time due to biofouling clogging pipes and pumps (Kangas and Adey, 2008). Using an array of hydraulic actuator pumps placed at the corners of a cubic tank, Webster et al. (2004) produced near-isotropic homogeneous turbulence comparing the flow characteristics with other studies using grids. The absence of moving structures inside the tank not only facilitates current measurements but also reduced the risk of mechanically damaging the organisms. Subsurface pumps can also be used to simulate surface wind-waves within a tank (Zhou et al., 2016). Laboratory flume tanks also use pump systems to produce specific flow regimes, generating a variety of ε under both laminar and turbulent regimes. A number of studies were carried out on different bioluminescent dinoflagellates to ascertain the threshold shear required to make them bioluminesce (Rohr et al., 1990; Latz and Rohr, 1999; Latz et al., 2004; Latz et al., 2009). Once this relationship has been determined, this threshold can be used to calculate the turbulence by recording the bioluminescence intensity. By using aerofoils in a flume tank, Laws et al. (1983) promoted turbulence eddies; as water moves at a critical flow velocity over the aerofoils, pressure differentials above and below produce turbulent vortices resulting in a yield doubling of the diatom *Phaeodactylum tricornutum* Bohlin.

Magnetic stirrers: Magnetic stirring devices are commonly used to agitate chemical solutions. The resulting turbulence profile produced in a vessel is inverted when compared to those in nature.

Typically, a water column will exhibit a wind- and convection-mixed turbulent upper layer with ε decreasing with depth. Large flows can cause mixing at depth via bed friction which can result in high levels of turbulence. However, this would need to occur in a water column that is suitably shallow enough to allow this bottom-generated turbulence to propagate up into the photic layer for this to be applicable within a cosm context. In addition, the turbulence field generated from magnetic stirrers is difficult to measure accurately so any biological changes are difficult to attribute to a particular flow characteristic (Warnaars et al., 2006). Researching optimal growth conditions for the dinoflagellate *Crypthecodinium cohnii*, Tuttle and Loeblich (1975) compared cell growth from cultures subjected to rotary shakers and magnetic stirrers before concluding that the shaker intensities used in the experiment damaged cells with no significant increase in growth compared to cultures exposed to magnetic stirring.

Rotating chambers: An enclosed chamber can be constructed that rotates in the z-axis. This technique is useful when studying the effects of vertical mixing especially on species that exhibit gravitaxis or have a preferential swimming / buoyancy direction. Sengupta et al. (2017) made use of a space-saving and cost-effective turbulence generation technique via a millimetre-scale "millifluidic chamber". Attached to a computer-controlled motor, the chamber could be programmed to mimic vertical overturning, specifically designed to be the same order of magnitude as Kolmorogov scale overturns.

Wave tanks: As with flume tanks, many laboratories now also have separate wave tanks or the ability to convert an existing flume tank. It can be difficult to directly measure the turbulent field associated with wave events due to surface oscillations and cavitation which interfere with velocity probes that need to be constantly submerged. As such, Stokes et al. (2004) developed a novel technique utilising bioluminescent dinoflagellates to correlate the intensity of light emitted to ε within a wave. Waves were computer-generated to consistently break at the same location while a

slow-motion digital camera was used to photograph the breaker with pixel light intensity of the image being related to the shear stress the organism was subjected to.

Impellers/propellers: A benefit of using propellers to produce turbulence in the laboratory is that the equipment is relatively low-cost and off-the-shelf, coming in a variety of different sizes and materials. Furthermore, the propellers can be easily attached to variable speed motors to produce a range of turbulent intensities. The propeller / impellor can have a profound effect on the circulation within the tank with radial impellors (vertical blades attached to a horizontal disc) resulting in two pairs of convective cells while axial impellors (akin to a boat propeller) cause a single pair of convective cells. The impellors can be sized appropriately and spin at specific speeds to either promote tank circulation or to generate localised turbulence; Sanford (1997) recommends a balance between these two extremes. A propeller system was used by Garrison and Tang (2014) to test the effect of high intensity episodic turbulence on diatoms noting an increase in cell mortality after exposure of only 45 seconds. Impellor like-structures have been used in a number of longer-duration multi-trophic experiments involving natural populations of phytoplankton and zooplankton (Donaghay and Klos, 1985; Escaravage et al., 1997; Petersen et al., 1998). These set-ups involve a central shaft with rods / paddles attached at specific depths to promote vertical stratification with separate well-mixed layers mirroring an upper wind-mixed layer with a lower mixed layer. The rotational direction is alternated to prevent whirlpool mixing that would transfer water from one layer to another. In order to simulate a reduction in flow that would normally be associated with tidal slack, Petersen et al. (1998) stopped the rotational mixing periodically. Donaghay and Klos (1985) used a variety of horizontal paddles at different depths to produce two separate well-mixed layers; a physical regime found in nature that is difficult to replicate using other methods of turbulence generation.

Paddles: Mechanised paddles can be placed into a cosm with the size, orientation and placement of the paddles altered at the discretion of the researcher. The paddles can oscillate horizontally or

vertically with the agitation produced increasing with distance from the pivot. As such, it may be prudent to opt for a rotating paddle (analogous to a watermill wheel) to ensure more isotropic conditions (Richmond and Vonshak, 1978; Dempsey, 1982).

Dialysis cylinders: Analogous to a small limnocorral, Köhler (1997) placed a natural population of phytoplankton into a 650ml transparent cylinder and suspended it into various aquatic environments. Using a lift system, the cylinder was suspended at depth and oscillated vertically through the water column at various amplitudes, frequencies and durations to mirror natural vertical mixing. The water within the cylinder was homogenised via a single paddle mounted on the inner edge of the cylinder, mixing the internal fluid as the cylinder rolled.

Convective mixing: It is possible to generate convective mixing within a cosm by either applying a heat source at the base (causing the water to rise) or by cooling the surface (causing the water to sink). The convective cell(s) established can be described as a function of water depth and the temperature difference between the top and bottom of the tank; high temperatures on the surface reducing to lower temperatures at depth will clearly result in a classic stratified water column with a distinct thermocline. Inverting this set-up by cooling the surface water and gently heating the water depth will result in a constant thermal instability mimicking the advection of water akin to a turbulent overturn. If carried out in suitably sized cosms (of the scale of natural turbulent overturns), this technique generates vertical turbulent overturns that more closely match those found in nature. Thus, the light climate that the planktonic organisms experience would be more realistic with regards to vertical distances moved. Båmstedt and Larsson (2018) showcased the convective-mixing abilities of the cosm facilities at Umeå Marine Science Centre, Sweden. Each 5m-high mesocosm is surrounded by three vertical sections into which flows a solution which can be heated or cooled to produce specific temperature profiles. This can be used to replicate the natural thermoclinic temperature structures, but by inverting the temperature profile via mild heating at

depth, it is possible to cause convective overturning. A larger temperature difference between the top section and the lower section causes a greater degree of convective flow.

APPENDIX 2 - Lesser-used techniques for quantifying turbulence

Dye dispersion: Dye tracing involves the release of a fluorescent dye product into a mesocosm in order to approximate turbulent mixing. The dye is released at mid-depths and then monitored by either taking water samples at depth, by pumping water at depth through a surface fluorometer or by conducting fluorimetry profiles with depth. Working on the CEPEX array, Steele et al. (1977) used dye dispersion to quantify vertical diffusivity for a number of mesocosm studies (Eppley et al., 1978; Sonntag and Parsons, 1979). By measuring the vertical distribution of the dye with time, Steele et al. (1977) were able to not only observe the gradual homogenisation of the dye concentration but also observed the development of a secondary patch of dye concentration at depth.

Clearly the dye substance that is used to measure flow should be inert so as to not react with any surfaces / materials within the tank. Furthermore, the substance should not be toxic nor should it act as or decay into a chemical species that could influence growth rate of any phytoplankton / bacteria within the experiment. For example, Båmstedt and Larsson (2018) introduced humic acid as a marker dispersant in their initial mixing studies before switching to rhodamine dye. Humic acid can decompose into other bioactive compounds / nutrients so could influence phytoplankton growth with time. Furthermore, the addition of an acid would alter the gas solubility of the water as well as biasing any biological experiment towards low-pH tolerant species. At high concentrations, rhodamine dye would affect light transmission through the water especially towards the UV end of the spectrum.

Bioluminescence: Certain species of dinoflagellates are known to exhibit bioluminescence, producing a brilliant blue light when exposed to species-dependent shear flows. As well as flow regime, dinoflagellate cells have been shown to exhibit bioluminescent tendencies under a variety of rapidly changing factors including thermal, pH, chemical, electrical and osmotic pressure (see

references in Stokes et al. (2004)). While this technique is applicable to flow visualisation in turbulent fields, it is restricted to studies of bioluminescent organisms alone. It is not recommended to add bioluminescent organisms to cosms with other species present as this would bias the population dynamics considerably. Firstly, a number of bioluminescent species are allelopathic, producing toxins that impede motility, growth rates and nutrient uptake rates (Schwartz et al., 2016). Other species, such as *Noctiluca scintillans* (Macartney) Kofoid & Swezy, are carnivorous so would skew population growth measurements via grazing. Furthermore, carnivorous dinoflagellates of this type excrete ammonia which can cause subsequent growth rate changes in different groups (Turkoglu, 2013).

Using colonies of *Pyrocystis fusiformis* C.W.Thomson, Stokes et al. (2004) used a wave tank and an intensified slow-motion camera to record the light emitted by the cells in a breaking wave. Firstly, the cell anxiety parameter for the species is calculated from observations; this factor is an inherent property of the cell which dictates the likelihood that the cell will emit light given a certain environmental perturbation. The pixel intensity is recorded then used to estimate the local shear stress in the fluid medium which can then be converted into shear stress values and ε. The digital images produced are effectively 2D maps showing the quantitative evolution of a breaking wave with time.

While this technique can be used to quickly produce a spatial map of ε, it does come with some bias namely the presence of bubbles which scatter / absorb the emitted light. It is possible to omit the effects of bubbles by subtracting the mean intensity recorded in a process known as thresholding. Thresholding itself is a subjective process so it is crucial that the same threshold level is applied to all images. The images can be adjusted so as to remove light occurring outside of the perturbation (e.g. behind the breaking wave) and those that exhibit radically different light properties. It is proposed to use a light source of known intensity placed in the sample region so as to properly account for the scattering / absorption effects of bubbles. Another factor to consider is that of cell

memory; a measure of how the cells may adapt to the conditions they are being exposed to and alter their light emission accordingly (Stokes et al., 2004). As well as wave tanks, flume tanks have also been used in studies where the response of a given bioluminescent species can be monitored with regards to different flow rate shear stresses under both laminar and turbulent regimes (Rohr et al., 1990; Latz and Rohr, 1999).

Depending on the level of ε encountered, it is possible to use different bioluminescent species that exhibit different trigger thresholds. In an experiment aiming to observe laminar and turbulent flow in pipes, Latz et al. (2004) experimented with four different dinoflagellate species with the aim of producing a shear sensitivity hierarchy. As well as exhibiting shear thresholds ranging across an order of magnitude, the cells also display a range of morphological differences being fusiform, spherical and spined. As the flow rate in the pipe apparatus was altered in the presence of the different species, light flashes were recorded using a photon-counting photomultiplier system.

APPENDIX 3 - Summary table of known phytoplankton-turbulence experiments

Turbulence Method	**Cosm material**	**Approx. cosm volume (m^3)**	**Organism(s)**	**Turbulence Dissipation Rate Range (m^2/s^3) (or equivalent parameter)**	**Reference**
Aeration	Glass	2.5×10^{-3}	Green algae – *Dunaliella viridis* Teodoresco	6.8×10^{-5} to 4.8×10^{-3}	Aguilera et al. (1994)
Aeration	Glass	1.0×10^{-3}	Green algae – *Scenedesmus obliquus* (Turpin) Kützing, *Stichococcus* sp.	None	Bakus (1973)
Aeration	Unspecified	2.5×10^{-2}	Natural population including: Diatoms: *Skeletonema costatum* (Greville) Cleve, *Chaetoceros* sp., *Lauderia* sp., *Thalassiosira cf. hyalina* (Grunow) Gran, *Thalassiosira cf. allenii* H.Takano, *Pseudonitzschia* sp, *Guinardia* sp.,	10^{-3} to 10^{-1}	Cózar and Echevarría (2005)

Aeration	Polyethylene	6.65×10^{1}	Natural population including: Diatoms – *Chaetoceros socialis* H.S.Lauder, S*tephanopyxis palmeriana* (Greville) Grunow, *Pseudo-nitzschia pungens* (Grunow ex Cleve) Hasle [a], *Coscinodiscus wailesii* Gran & Angst Dinoflagellates - *Dinophysis* sp., *Amphidinium* sp., *Peridinium* sp., *Gymnodinium* sp., *Noctiluca* sp. Ciliates – *Eutintinnus pectinis* Kofoid & Campbell, *Favella ehrenbergii* (Claparède & Lachmann) Jörgensen, *Helicostomella subulate* (Ehrenberg) Jörgensen, *Salpingella curta* Kofoid & Campbell Copepods - various	2.15×10^{-9} to 2.51×10^{-8}	Eppley et al. (1978)
Aeration	Glass	1.0×10^{-3}	Ciliates – *Tetrahymena pyriformis* (Ehrenberg), *T. thermophila, T. pigmentosa*	None	Hellung-Larsen and Lyhne (1992)

Aeration	Unknown	Unknown	Diatoms - *Chaetoceros curvisetus* Cleve, *Skeletonema costatum*	None	Schöne (1970)
Aeration	Polyethylene	1.67 x 10^3	Natural population of phytoplankton & zooplankton with salmonids added artificially. Phytoplanktonic species unspecified but main group enumerated.	Vertical eddy diffusivity coefficient = 0.06cm^2/s (Steele et al., 1977).	Sonntag and Parsons (1979)
Aeration	Acrylate	3.4 x 10^{-3}	Diatom – *Phaeodactylum tricornutum*	None	Thomas et al. (1984a)
Aeration	Acrylate	3.4 x 10^{-3}	Green algae – *Dunaliella primolecta* Butcher & *Tetraselmis suecica* Butcher.	None	Thomas et al. (1984b)
Aeration	Acrylate	3.4 x 10^{-3}	Golden algae - *Isochrysis* (Tahitian strain) & *Microchloropsis salina* (D.J.Hibbard) M.W.Fawley, I.Jameson & K.P.Fawley [b]	None	Thomas et al. (1984c)
Aeration	Glass	4.0 x 10^{-5}	Dinoflagellate – *Crypthecodinium cohnii*	None	Tuttle and Loeblich (1975)
Convective heating	Polyethylene	2.03 x 10^0	None	Dye injection homogenisation timed	Båmstedt and Larsson (2018)

Couette	Unspecified	1.00 x 10^{-3}	Diatom - *Skeletonema* sp., *Chaetoceros* sp.	Converted using Equation (6) 3.42 x 10^{-5}	Bergkvist et al. (2018)
Couette	Unknown	Unknown	Dinoflagellate - *Alexandrium minutum* Halim	1.64 x 10^{-2} (Berdalet et al., 2007)	Chen et al. (1998)
Couette	Acrylate / steel	4.16 x 10^{-4}	Green algae - *Chlorella* sp.	Converted using Equation (6) 1.28 x 10^{-2}	Davis et al. (1953)
Couette	Glass	8.78 x 10^{-4}	Dinoflagellate – *Lingulodinium polyedra* [c]	Converted using Equation (6) 7.96 x 10^{-9} to 1.82 x 10^{-3}	Gibson and Thomas (1995)
Couette	Unspecified	8.79 x 10^{-4}	Green algae – *Desmodesmus communis* (E.Hegewald) E.Hegewald [k]	1.27 x 10^{-3} to 3.13 x 10^{-1}	Hondzo et al. (1997)
Couette	Glass	1.56 x 10^{-4}	Dinoflagellate – *Lingulodinium polyedra* [c]	1.00 x 10^{-5} to 3.50 x 10^{-4}	Juhl and Latz (2002)
Couette	Glass	1.56 x 10^{-4}	Dinoflagellate – *Lingulodinium polyedra* [c]	Converted using Equation (6) 1.88 x 10^{-5}	Juhl et al. (2000)
Couette	Acrylate	3.91 x 10^{-4}	Dinoflagellate – *Alexandrium catenella* (Whedon & Kofoid) Balech [d]	1.0 x 10^{-5}	Juhl et al. (2001)

Couette	Acrylate	8.0×10^{-4}	Diatoms - *Skeletonema costatum, Thalassiosira nordenskioeldii* P.T. Cleve	2.5×10^{-7}	Karp-Boss and Jumars (1998)
Couette	Acrylate	8.0×10^{-4}	Dinoflagellates - *Glenodinium foliaceum* F.Stein, *Alexandrium catenella* [d]	1.0×10^{-8} to 1.0×10^{-5}	Karp-Boss et al. (2000)
Couette	Acrylate	2.38×10^{-4}	Dinoflagellates – *Lingulodinium polyedra* [c], *Pyrocystis noctiluca* Murray ex Haeckel, *P. fusiformis*	Converted using Equation (6) Large tanks = 9.65×10^{-4} to 6.86×10^{-1} Small tanks = 3.86×10^{-3} to 2.75×10^{0}	Latz et al. (1994)
Couette	Unspecified	1.23×10^{-3}	Cyanobacteria – *Nodularia sphaerocarpa* Bornet & Flahault, *N. spumigena* Mertens ex Bornet & Flahault	4.66×10^{-6} to 3.23×10^{-4}	Moisander et al. (2002)
Couette	Acrylate	6.45×10^{-4}	Diatom – *Ditylum brightwellii* (T.West) Grunow	5.94×10^{-11} to 5.0×10^{-8}	Pasciak and Gavis (1975)
Couette	Polycarbonate	1.51×10^{-4}	Dinoflagellate – *Pfiesteria piscicida* Steidinger & J.M.Burkholder with cryptophyte food source *Storeatula major* D.R.A.Hill	2.38×10^{-10} to 2.88×10^{-8}	Stoecker et al. (2006)

Couette	Glass	6.45 x 10^{-4}	Dinoflagellate – *Lingulodinium polyedra* [c]	4.50 x 10^{-6} to 1.64 x 10^{-2}	Thomas and Gibson (1990a)
Couette	Glass	6.45 x 10^{-4}	Dinoflagellate – *Lingulodinium polyedra* [c]	1.80 x 10^{-5} to 1.64 x 10^{-2}	Thomas and Gibson (1990b)
Couette	Glass	Unspecified	Dinoflagellate – *Akashiwo sanguinea* [e]	2.8 x 10^{-7} to 1.8 x 10^{-3}	Thomas and Gibson (1992)
Couette	Unknown	Unknown	Dinoflagellates – *Akashiwo sanguinea* [e], *Prorocentrum micans* Ehrenberg	4.6 x 10^{-4} (Berdalet et al., 2007)	Tynan (1993)
Dialysis chamber	Glass	6.5 x 10^{-4}	Natural population including: Diatom – *Scenedesmus* sp., *Cymbella* sp. *Navicula* sp., *Diatoma* sp. Green Algae – *Chlamydomonas* sp. Cryptophyte – *Cryptomonas* sp.	None	Köhler (1997)

Grid - horizontal	Glass	4.9×10^{-3}	Green Algae – *Nephroselmis olivacea* F.Stein, *Cryptomonas curvata* Ehrenberg, *Spondylosium pulchellum* (W.Archer) W.Archer, *Pediastrum boryanum* (Turpin) Meneghini Diatoms – *Asterionella formosa* Hassall, *Aulacoseira granulata* (Ehrenberg) Simonsen	7.9×10^{-5} to 7.8×10^{-3}	Fraisse et al. (2015)
Grid - horizontal	Acrylate	9.28×10^{-4}	Dinoflagellate – *Heterosigma akashiwo* (Y.Hada) Y.Hada ex Y.Hara & M.Chihara	2.0×10^{-9} to 1.6×10^{-8}	Linares (2015)
Grid - horizontal	Unspecified	6.65×10^{-3}	Dinoflagellate – *Phaeocystis globosa*	1.0×10^{-6} to 1.0×10^{-4}	Schapira et al. (2006)
Grid - horizontal	Acrylate	3.05×10^{-2}	Green algae – *Selenastrum capricornutum*	9.60×10^{-9} to 1.25×10^{-6}	Warnaars et al. (2006)
Grid - vertical	Acrylate	3.0×10^{-2}	Natural population with a focus on phytoplankton biomass and copepod *Acartia italica* Steuer	Vertical eddy diffusivity = 0.5 cm^2/s (unstirred) / 1 to 5 cm^2/s (stirred).	Alcaraz et al. (1988)
Grid - vertical	Acrylate	2.92×10^{-1}	Marine snow – Diatom aggregates of *Chaetoceros* sp. and *Nitzschia* sp.	1.0×10^{-7} to 1.0×10^{-4}	Alldredge et al. (1990)

Grid - vertical	Acrylate	1.5 x 10^{-2}	Natural population (filtered through a 150 µm mesh) including: Bacteria – *Synechococcus* sp., *Prochlorococcus* sp.	5.5 x 10^{-6}	Arin et al. (2002);
Grid - vertical	Acrylate	1.5 x 10^{-2}	Natural population (filtered through a 150 µm mesh) including: Diatoms – *Chaetoceros* sp, *Pseudo-nitzschia* sp	5.5 x 10^{-6}	Maar et al. (2002)
Grid - vertical	Acrylate	2.60 x 10^{0}	Natural population (filtered through 250µm filter) including: Diatoms - *Chaetoceros* sp., *Cylindrotheca closterium* (Ehrenberg) Reimann & J.C.Lewin, *Dactyliosolen fragilissimus* (Bergon) Hasle, *Nitzschia longissima* (Brébisson) Ralfs, *Skeletonema costatum, Thalassiosira* sp.	2.0 x 10^{-9} to 1.0 x 10^{-4}	Beauvais et al. (2006)
Grid - vertical	Glass	1.0 x 10^{-3}	Dinoflagellates – *Akashiwo sanguinea* [e]	2.0 x 10^{-3}	Berdalet (1992)
Grid - vertical	Glass	4.0 x 10^{-3}	Dinoflagellates - *Alexandrium minitum, Akashiwo sanguinea* [e]	1 x 10^{-4}	Berdalet and Estrada (1993)

Grid- vertical	Acrylate	1.38×10^{-2}	Bacteria – *Vibrio splendidus* Flagellate – *Paraphysomonas* sp.	1.00×10^{-5} to 1.35×10^{-5}	Delaney (2003)
Grid - vertical	Acrylate	2.0×10^{-3}	Ciliate – *Strombidium sulcatum* Claparède & Lachmann	5.0×10^{-7} to 2.0×10^{-4}	Dolan et al. (2003)
Grid - vertical	Acrylate	3.0×10^{-2}	Natural population including: Diatoms – *Chaetoceros* sp., *Thalassiosira* sp., *Leptocylindrus danicus* Cleve, *Skeletonema costatum, Cylindrotheca closterium* Dinoflagellates – *Protoperidinium* sp, *Scrippsiella trochoidea* (F.Stein) A.R.Loeblich III Haptophyte – *Emiliania huxleyi* (Lohmann) W.W.Hay & H.P.Mohler	Vertical eddy diffusivity = 0.5 cm^2/s (unstirred) / 1 to 5 cm^2/s (stirred).	Estrada et al. (1987)

Grid - vertical	Polyethylene	2.50×10^{0}	Natural population filtered through 250µm filter including: *Chaetoceros* sp., *Cylindotheca closterium, Dactyliosolen fragilissimus, Nitzschia longissima, Skeletonema costatum, Thalassiosira* sp. (Beauvais et al., 2006)	1.0×10^{-7} to 1.0×10^{-6}	(Guadayol et al., 2009a)
Grid - vertical	Acrylate	2.0×10^{-3}	Dinoflagellate – *Oxyrrhis marina* Dujardin Haptophyte – *Isochrysis sp.*	1.0×10^{-8} to 1.0×10^{-4}	Havskum (2003)
Grid - vertical	Acrylate	2.0×10^{-3}	Dinoflagellate – *Kryptoperidinium triquetrum* (Ehrenberg) U.Tillmann, M. Gottschling, M.Elbrächter, W.-H.Kusber & M.Hoppenrath [f]	1.0×10^{-8} to 1.0×10^{-4}	Havskum and Hansen (2006)
Grid - vertical	Acrylate	2.0×10^{-3}	Dinoflagellates – *Fragilidium subglobosum* & *Tripos muelleri* Bory [g]	1.0×10^{-8} to 1.0×10^{-4}	Havskum et al. (2005)
Grid - vertical	Fibreglass	3.02E+00	Natural population (phytoplankton dominated by *Anabaena* sp.)	2.0×10^{-4} to 3.80×10^{-3}	Howarth et al. (1993)
Grid - vertical	Acrylate	2.60×10^{0}	see Beauvais et al. (2006)	2.0×10^{-9} to 1.0×10^{-4}	Iversen et al. (2009)

Grid - vertical	Unspecified	Unspecified	Dinoflagellates – *Peridiniella danica* (Paulsen) Y.B.Okolodkov & J.D.Dodge*, Gyrodinium dominans* Hulbert*, Oxyrrhis marina* Ciliate – *Mesodinium pulex* Claparède & Lachmann	1.2×10^{-6}	Martínez et al. (2017)
Grid - vertical	Unspecified	2.40×10^{0}	Natural population filtered through 250µm filter – no specific species reported.	1.0×10^{-7} to 1.0×10^{-4}	Metcalfe et al. (2004)
Grid - vertical	Polyethylene	2.70×10^{1}	Natural plankton population including: Flagellate – *Ebria tripartita* (Schumann) Lemmermann Diatom – *Skeletonema costatum* Ciliate – *Mesodinium rubrum* (Lohmann) Leegard, *Cyclotrichium* sp. Copepods – *Calanus helgolandicus* Claus*, Calanus finmarchicus* Gunnerus	5.3×10^{-9} to 1.7×10^{-7} (Svensen et al., 2001)	Nejstgaard et al. (2001a)

Grid - vertical	Polyethylene	2.70 x 10^{1}	Natural plankton population including: Flagellate – *Octactis speculum* (Ehrenberg) F.H.Chang, J.M.Grieve & J.E.Sutherland [i], *Emiliania huxleyi, Ebria tripartita* Diatom – *Skeletonema costatum, Amphiprora sp* Ciliates – *Strombidium* spp. and *Strombilidium* spp. Copepods – *Calanus helgolandicus*	5.3 x 10^{-9} to 1.7 x 10^{-7} (Nerheim et al., 2002)	Nejstgaard et al. (2001b)

Grid - vertical	Unspecified	1.30×10^{1}	Natural population including: Dinoflagellates – *Peridinium* sp. Diatoms – *Skeletonema costatum, Chaetoceros compressus* Lauder*, Chaetoceros affinis* Lauder*, Chaetoceros didymus* Ehrenberg*, Chaetoceros perpusillus* Cleve*, Cylindrotheca fusiformis* Reimann & J.C.Lewin*, Leptocylindricus danicus* Cleve*, Rhizosolenia delicatula* Cleve Golden Algae – *Dinobyron* sp. Copepods - various	None	Oviatt (1981)
Grid - vertical	Glass	1.0×10^{-4}	Flagellate – *Paraphysomonas imperforata* I.A.N.Lucas	8.5×10^{-5} to 8.6×10^{-1}	Peters and Gross (1994)
Grid - vertical	Glass	1.0×10^{-4}	Flagellate – *Paraphysomonas imperforata*	5.0×10^{-6} to 1.5×10^{-3}	Peters et al. (1996)
Grid - vertical	Acrylate	1.5×10^{-2}	Natural population – no species identified but groups of bacteria, flagellates and ciliates.	5.3×10^{-6} to 5.9×10^{-6}	Peters et al. (2002)

Grid - vertical	Acrylate	1.7 x 10^{-2}	Cyanobacteria – *Microcystis aeruginosa* (Kützing) Kützing	Turbulent intensity ranged from 7.1 x 10^{-3} and 7.04 x 10^{-2} m/s	Regel et al. (2004)
Grid - vertical	Glass	2.5 x 10^{-2}	Diatom – *Phaeodactylum tricornutum.* Dinoflagellate – *Brachiomonas submarina* Bohlin	2.3 x 10^{-4} to 2.3 x 10^{-1}	Savidge (1981)
Grid - vertical	Polycarbonate	1.2 x 10^{-2}	Dinoflagellates – *Alexandrium catenella* [d], *A. tamarense* [h], *Tripos fusus* (Ehrenberg) F.Gómez [j], *Tripos muelleri* [g], *Gymnodinium catenatum* H.W.Graham, *Gyrodinium sp., Lingulodinium polyedra* [c], *Pyrocystis fusiformis, P. noctiluca*	1.0 x 10^{-8} to 1.0 x 10^{-4}	Sullivan and Swift (2003)

Grid - vertical	Polyethylene	2.70 x 10^{1}	Diatoms – *Chaetoceros socialis* Flagellates – *Resultor micron* (Throndsen) Moestrup, *Nephroselmis minuta* (N.Carter) Butcher Haptophytes – *Phaeocystis pouchetii* (Hariot) Lagerheim Dinoflagellates - unspecified	5.3 x 10^{-9} to 1.9 x 10^{-7}	Svensen et al. (2001)
Inversion	Acrylate	7.68 x 10^{-8}	Raphidophyte – *Heterosigma akashiwo* (primarily)	3.0 x 10^{-8}	Sengupta et al. (2017)
Magnetic	Glass	1.0 x 10^{-4}	Dinoflagellates – *Scrippsiella lachrymosa* J.Lewis ex Head	None	Smith and Persson (2005)
Magnetic	Glass	4.0 x 10^{-5}	Dinoflagellate – *Crypthecodinium cohnii*	None	Tuttle and Loeblich (1975)
Paddles	Unspecified	Unspecified	Dinoflagellate – *Kryptoperidinium triquetrum* [f], *Alexandrium tamarense* [h] Diatom – *Skeletonema costatum*	1.0 x 10^{-5}	Dempsey (1982)

Paddles	PVC	1.30×10^{1}	Natural population including: Diatom – *Skeletonema costatum* Zooplankton – various copepods	None	Donaghay and Klos (1985)
Paddles	Glass	3.78×10^{-2}	Diatom – *Thalassiosira weissflogii* (Grunow) G.A.Fryxell and Hasle*, Skeletonema costatum* Cryptomonad – *Rhodomonas salina* (Wislouch) D.R.A.Hill & R.Wetherbee Chlorophyte – *Dunaliella tertiolecta* Butcher	1.1×10^{-4} to 4.0×10^{-4}	Garrison and Tang (2014)
Paddles	Acrylate	1.3×10^{-1}	Natural population including: Cyanobacteria - *Oscillatoria* spp, *Prochlorothrix hollandica* Burger-Wiersma, Stal & Mur	None	Kromkamp et al. (1992)
Paddles	Fibreglass	1.00E+00	Natural population – no species identified but chlorophyll-a and other pigments used to quantify populations of diatoms, cyanobacteria and cryptophytes.	3.00×10^{-7} to 6.89×10^{-5}	Petersen et al. (1998)
Paddles	Natural	Unspecified	Cyanobacteria – *Arthrospira* sp. (aka *Spirulina*)	None	Richmond and Vonshak (1978)

Paddles	Acrylate	1.3 x 10^{-1}	Cyanobacteria – *Prochlorothrix hollandica*	None	Rijkeboer et al. (1990)
Paddles	Unknown	Unknown	Diatoms - *Asterionellopsis glacialis* (Castracane) Round, *Skeletonema costatum*	Unknown	Thomas et al. (1997)
Pumping	Acrylate	7.5 x 10^{-2}	Dinoflagellates - *Lingulodinium polyedra* [c]	Shear stress ranged from 0.2 N/m^2 to 10 N/m^2	Latz and Rohr (1999)
Pumping	Acrylate	7.5 x 10^{-2}	Dinoflagellates – *Tripos fusus* [j], *Ceratocorys horrida, Lingulodinium polyedra* [c], *Pyrocystis fusiformis*	Shear stress ranged from 0.2 N/m^2 to 10 N/m^2	Latz et al. (2004)
Pumping	Fibreglass	4.15 x 10^{0}	Diatom – *Phaeodactylum tricornutum*	Shear stress ranged from 0.02 N/m^2 to 0.3 N/m^2	Laws et al. (1983)
Pumping	Acrylate	5.0 x 10^{-2}	Natural plankton population including: Cyanobacteria - *Limnothrix* sp., *Aphanizomenon* sp. Yellow-green algae - *Tribonema* sp. Green algae - *Closterium* sp., *Monoraphidium* sp.	Flow of 2.5 mL/s resulting in a mean upward velocity of 7.6 ± 1.4 mm/s.	Pannard et al. (2007)

Pumping	Steel	7.5×10^{-2}	Dinoflagellates – *Lingulodinium polyedra* [c], *Tripos fusus* [j], and *Protoperidinium* sp.	5.3×10^{-9} to 1.7×10^{-7}	Rohr et al. (1990)
Pumping	Steel	7.5×10^{-2}	Dinoflagellates – *Lingulodinium polyedra* [c], *Tripos fusus* [j], and *Protoperidinium* sp.	5.3×10^{-9} to 1.7×10^{-7}	Rohr et al. (1997)
Pumping	Steel	4.5×10^{-1}	Dinoflagellates – *Lingulodinium polyedra* [c], *Tripos fusus* [j], and *Protoperidinium* sp.	Mean shear stress = 11 to 13.5 dyn/cm^2	Rohr et al. (2002)
Shaker - unspecified	Glass	2.5×10^{-3}	Diatom – *Chaetoceras affinis*	None	Talling (1960)
Shaker - orbital	Glass	3.0×10^{-3}	Dinoflagellates – *Akashiwo sanguinea* [e]	2.0×10^{-3}	Berdalet (1992)
Shaker - orbital	Glass	4.0×10^{-3}	Dinoflagellates - *Scrippsiella trochoidea, Prorocentrum micans*	2.0×10^{-4}	Berdalet and Estrada (1993)
Shaker - orbital	Glass	3.0×10^{-3}	Dinoflagellates – *Gymnodinium sp., Alexandrium minutum, Prorocentrum triestinum* J.Schiller	2.7×10^{-5} to 2.4×10^{-3}	Berdalet et al. (2007)
Shaker - orbital	Glass	1.0×10^{-4}	Cyanobacteria – *Anabaena cylindrica*	None	Fogg and Than-Tun (1960)

Shaker - orbital	Glass / polycarbonate	3.00 x 10^{-3}	None	1 x 10^{-10} to 1 x 10^{-2}	Guadayol et al. (2009b)
Shaker - orbital	Glass	2.5 x 10^{-5}	Ciliates – *Tetrahymena pyriformis, T. thermophile, T. pigmentosa*	1.17 x 10^{-2} to 2.16 x 10^{-2}	Hellung-Larsen and Lyhne (1992)
Shaker - orbital	Glass	3 x 10^{-3}	Dinoflagellates - *Prorocentrum micans, Scrippsiella trochoidea, Alexandrium minutum*	2.7 x 10^{-3}	Llaveria et al. (2010)
Shaker - orbital	Glass	1.0 x 10^{-4}	Diatom – *Ditylum brightwellii*	None	Pasciak and Gavis (1975)
Shaker - orbital	Polycarbonate	2.5 x 10^{-3}	Diatoms – *Thalassiosira pseudonana* Hasle & Heimdal, *Coscinodiscus* sp	1.0 x 10^{-3}	Peters et al. (2006)
Shaker - orbital	Unspecified	Unspecified	Dinoflagellates – *Peridinium cinctum* (O.F.Müller) Ehrenberg	4.3 x 10^{-3}	Pollingher and Zemel (1981)
Shaker - orbital	Glass	2.5 x 10^{-4}	Dinoflagellate – *Lingulodinium polyedra* [c]	2.0 x 10^{-2}	Thomas and Gibson (1990b)
Shaker - orbital	Glass	4.0 x 10^{-5}	Dinoflagellate – *Crypthecodinium cohnii*	None	Tuttle and Loeblich (1975)

Shaker - orbital	Glass	5.0×10^{-5}	Dinoflagellates – *Alexandrium tamarense* [h]	4.30×10^{-3} to 1.19×10^{-2}	White (1976)
Shaker - orbital	Glass	6.0×10^{-5}	Dinoflagellates – *Crypthecodinium cohnii*; *Kryptoperidinium triquetrum* [f]	1.0×10^{-5} to 9.9×10^{-5}	Yeung and Wong (2003)
Shaker - orbital	Glass	6.0×10^{-5}	Dinoflagellates – *Crypthecodinium cohnii*; *Kryptoperidinium triquetrum* [f]	1.0×10^{-5} to 9.9×10^{-5}	Yeung et al. (2006)
Shaker - orbital	Glass	1.25×10^{-4}	Dinoflagellates - *Ceratocorys horrida*	1×10^{-5} to 1×10^{-4} (Berdalet et al., 2007)	Zirbel et al. (2000)
Shaker - reciprocal	Glass	2.5×10^{-5}	Ciliates – *Tetrahymena pyriformis, T. thermophile, T. pigmentosa*	1.17×10^{-2} to 2.16×10^{-2}	Hellung-Larsen and Lyhne (1992)
Shaker - reciprocal	Glass	2.6×10^{-4}	Dinoflagellate - *Lingulodinium polyedra* [c]	Estimated using Equation (2) ~10	Juhl and Latz (2002)
Wave	Unspecified	9.90×10^{0}	Dinoflagellate – *Pyrocystis fusiformis*	3.0×10^{-2} to 3.0×10^{1}	Stokes et al. (2004)

[a] The diatom *Pseudo-nitzschia pungens* (Grunow ex Cleve) Hasle 1993 was formerly referred to as *Nitzschia pungens* Grunow ex Cleve 1897.

[b] The golden alga *Microchloropsis salina* (D.J.Hibbard) M.W.Fawley, I.Jameson & K.P.Fawley 2015 was formerly referred to as *Monallantus salina* Bourrelly 1958.

[c] The dinoflagellate *Lingulodinium polyedra* (F.Stein) J.D.Dodge 2018 was formerly referred to as *L. polyedrum* Dodge 1989 & *Gonyaulax polyedra* Stein 1883.

[d] The dinoflagellate *Alexandrium catenella* (Whedon & Kofoid) Balech, 1985 was formerly referred to as *Alexandrium fundyense* Balech, 1985

[e] The dinoflagellate *Akashiwo sanguinea* (K. Hirasaka) Gert Hansen & Moestrup 2000 was formerly referred to as *Gymnodinium nelsonii* Martin 1929, *G. sanguineum* Hirasaka 1922 & *G. splendens* Lebour 1925.

[f] The dinoflagellate *Kryptoperidinium triquetrum* (Ehrenberg) U.Tillmann, M. Gottschling, M.Elbrächter, W.-H.Kusber & M.Hoppenrath 2019 was formerly referred to as *Heterocapsa triquetra* (Ehrenberg) F.Stein 1883.

[g] The dinoflagellate *Tripos muelleri* Bory 1826 was formerly referred to as *Ceratium tripos* (O.F.Müller) Nitzsch 1817.

[h] The dinoflagellate *Alexandrium tamarense* (Lebour) Balech 1995 was formerly referred to as *A. tamarensis* Balech 1992, *Gonyaulax excavata* Balech 1971 & *G. tamarensis* Lebour 1925.

[i] The flagellate *Octactis speculum* (Ehrenberg) F.H.Chang, J.M.Grieve & J.E.Sutherland 2017 was formerly referred to as *Dictyocha speculum* Ehrenberg 1839.

[j] The dinoflagellate *Tripos fusus* (Ehrenberg) F.Gómez 2013 was formerly referred to as *Ceratium fusus* (Ehrenberg) Dujardin 1841.

[k] The green alga *Desmodesmus communis* (E.Hegewald) E.Hegewald 2000 was formerly referred to as *Scenedesmus quadricauda* Chodat 1926

The presence of an ‘unknown’ indicates a paper that was not available; ‘unspecified’ indicates that this information was absence from the paper.